National Defence | Défense nationale

LABORATORY TESTING RESULTS FOR THE DREO EXPERIMENTAL MAWS TRANSCEIVER

UNLIMITED

by

L. Campbell, G. Rempel and R. Robinson

DEFENCE RESEARCH ESTABLISHMENT OTTAWA

REPORT N0. 1205

Canada

November 1993
Ottawa

National Defence   Défense nationale

LABORATORY TESTING RESULTS FOR THE DREO EXPERIMENTAL MAWS TRANSCEIVER

by

L. Campbell, G. Rempel and R. Robinson
Airborne Radar and Navigation Section
Radar and Space Division

DEFENCE RESEARCH ESTABLISHMENT OTTAWA
REPORT NO. 1205

PCN
021LA

November 1993
Ottawa

ABSTRACT

An experimental transceiver for a radar-based Missile Approach Warning System (MAWS) was developed at the Defence Research Establishment Ottawa to aid in studying the most effective techniques for design and implementation of such systems. With the help of Canadian industry, the experimental system was completed in November of 1992. The transceiver was designed for airborne use, and will be undergoing flight trials in 1994. The MAWS transceiver is an L-band pulse Doppler radar with frequency agility, multiple pulse repetition frequencies, and pulse coding capabilities.

The following report outlines laboratory tests conducted on the experimental DREO MAWS transceiver, and shows performance specifications achieved by the system. These tests were designed to verify critical parameters of the transceiver, while providing a broad base of information that will aid in interpreting data from future flight tests. As well, the information contained in this report serves as a foundation for evaluating improvements made through further design modifications.

RÉSUMÉ

Au Centre de recherche pour la défense à Ottawa (CRDO), nous avons développé un émetteur-récepteur expérimental pour un Système d'Alerte de Missiles (SALM), afin d' étudier les techniques les plus prometteuses pour la conception d'un SALM utilisant un radar. Avec l'aide de l'industrie canadienne, le système expérimental fut complété en novembre, 1992. Le système a été conçu pour une utilisation aéroportée. Il sera l'objet d'essais en vol en 1994. Le SALM est un radar Doppler à impulsions en bande L, avec agilité de fréquence, multiples fréquences de répétition de l'impulsion, et capacités de codage de l'impulsion.

Ce document décrit des tests en laboratoire de l'émetteur-récepteur du SALM et donne les performances du système. Ces tests ont été conduits dans le but de vérifier les paramètres critiques de l' émetteur-récepteur. Les resultats permettront également une meilleure interprétation de donneés futures, prises en vol. De plus, l'information de ce rapport servira de base pour évaluer les améliorations ultérieures.

EXECUTIVE SUMMARY

The results of recent conflicts have demonstrated the need to protect Canadian Forces fighter aircraft against the threat of incoming missiles. In particular, these aircraft are vulnerable to infrared guided missiles because they cannot be detected by onboard sensors such as radar warning receivers. In response to this need, an experimental transceiver for a Missile Approach Warning System (MAWS) was developed at the Defence Research Establishment Ottawa (DREO) to study the most effective techniques in the design and implementation of missile approach warning using radar. The experimental system was completed in November of 1992 under contract with MPB Technologies of Montreal. The system was designed for airborne use, and will be undergoing extensive flight trials in 1994.

The following report outlines laboratory tests conducted on the DREO MAWS transceiver, and shows the performance achieved by the system. These tests were designed to verify critical parameters of both the MAWS transceiver and an accompanying Controller/Data Acquisition (C/DAQU), while providing a broad base of information that will aid in interpreting data from future flight tests. As well, the information contained in this report serves as a foundation for evaluating improvements made through further design modifications. A measure of the system performance degradation in the less benign conditions of a flight trial is also possible through comparison with this data.

The MAWS transceiver is an L-band pulse Doppler radar with frequency agility, multiple pulse repetition frequencies (PRFs), and pulse coding capabilities. Initially, this airborne system will provide Canada with the capability to collect raw clutter data from a high-speed platform for analysis back in the laboratory. This clutter data will play a critical role in the development of detection algorithms, and may be implemented directly in a missile approach warning simulator.

TABLE OF CONTENTS

LIST OF FIGURES

LIST OF TABLES

1.0 INTRODUCTION

The results of recent conflicts have demonstrated the need to protect Canadian Forces fighter aircraft against the threat of incoming missiles. In particular, these aircraft are vulnerable to infrared guided missiles because these missiles cannot be detected by onboard sensors such as radar warning receivers. Systems exist today that are capable of protecting slower moving platforms such as helicopters and transport aircraft, but currently there are no systems that have proven to be effective for a fighter application. In response to this need, an experimental transceiver for a radar-based Missile Approach Warning System (MAWS) was developed at the Defence Research Establishment Ottawa (DREO) to aid in studying the most effective techniques for the design and implementation of such systems. The experimental transceiver was completed in November of 1992 under contract with MPB Technologies of Montreal [4, 5, 6, 7]. The transceiver was designed for airborne use, and will be undergoing flight trials in 1994.

The following report outlines laboratory tests conducted on the experimental DREO MAWS transceiver, and shows the performance achieved by the system. These laboratory testing techniques were designed to verify critical parameters of the MAWS transceiver, while providing a broad base of information that will aid in interpreting data from future flight tests. As well, the information contained in this report serves as a foundation for evaluating improvements made through further design modifications. Measurement of the system performance degradation in the less benign conditions of a flight trial will also be possible through comparison with this data.

The MAWS transceiver is an L-band pulse Doppler radar with frequency agility, multiple pulse repetition frequencies (PRFs), and pulse coding capabilities. Initially, this airborne transceiver will provide Canada with the capability to collect raw clutter data from a high-speed platform for analysis in the laboratory. This clutter data will play a critical role in the development of detection algorithms, and may be implemented directly in a MAWS simulator.

The transceiver is contained in two boxes. The first is an external payload assembly (EPA), which houses the solid state power amplifier and an initial amplification stage for the receive chain. The second is the cabin mounted equipment (CME) which houses the rest of the transceiver electronics. An accompanying Controller/Data Acquisition Unit (C/DAQU) box holds a VME chassis and boards, and Exabyte 8mm tape drives. A blade antenna will be mounted on the aircraft, and an LTN-91 Inertial Reference Unit will be connected to the C/DAQU to allow collection of flight parameters via an ARINC bus. The hardware, shown in Figure 1, was designed to conform to the size and weight specifications of the Institute for Aerospace Research (IAR) for experimental equipment flown aboard their T-33 jet. From left to right in Figure 1, the components are: the MAWS CME, the MAWS EPA, the MAWS Power and Signals Distribution Box, and the C/DAQU. In the foreground of Figure 1 are the Pilot Interface and the MAWS antenna. The system will undergo flight trials on the T-33 to collect clutter data under varying conditions and with different radar parameters. A simplified functional block diagram of the main channel of the transceiver is shown in Figure 2.

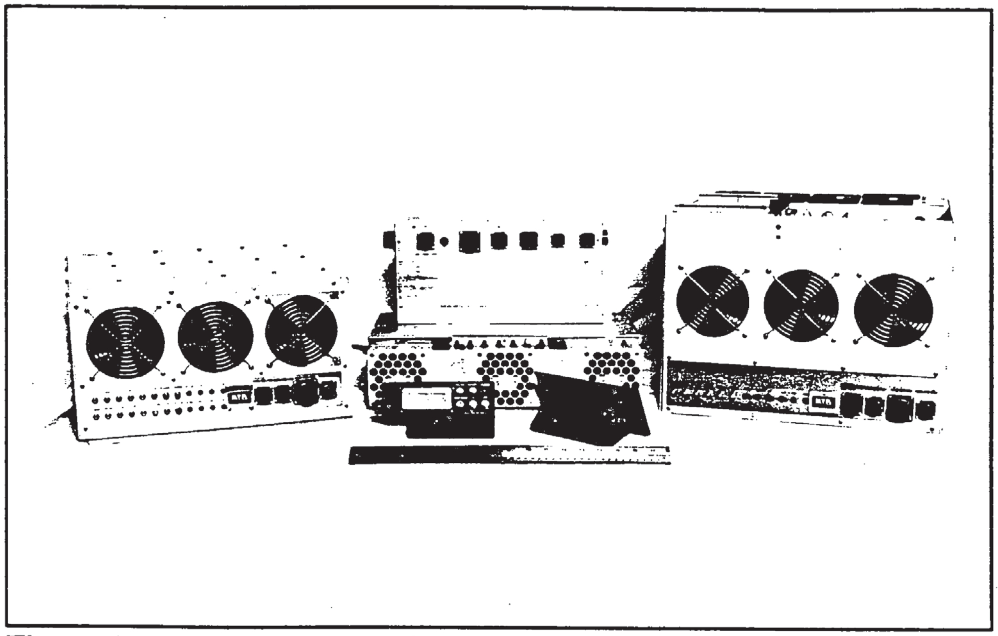

Figure 1 DREO MAWS Equipment.

The user can control the variable parameters of the MAWS system through a command file written on a 3 ½" floppy disk. The following parameters are programmable:

a. Frequency: 16 different frequencies from 1250-1400 MHz in increments of 10 MHz
b. Pulse Repetition Frequency: 40 or 50 kHz
c. Pulse Phase: 0-358.6° in steps of 1.40625°
d. Pulse Width: 1 μs or 3.3 μs
e. Burst length: 16 to 4080 pulses/burst
f. Collection of airborne platform data such as altitude, yaw, pitch and roll angles.

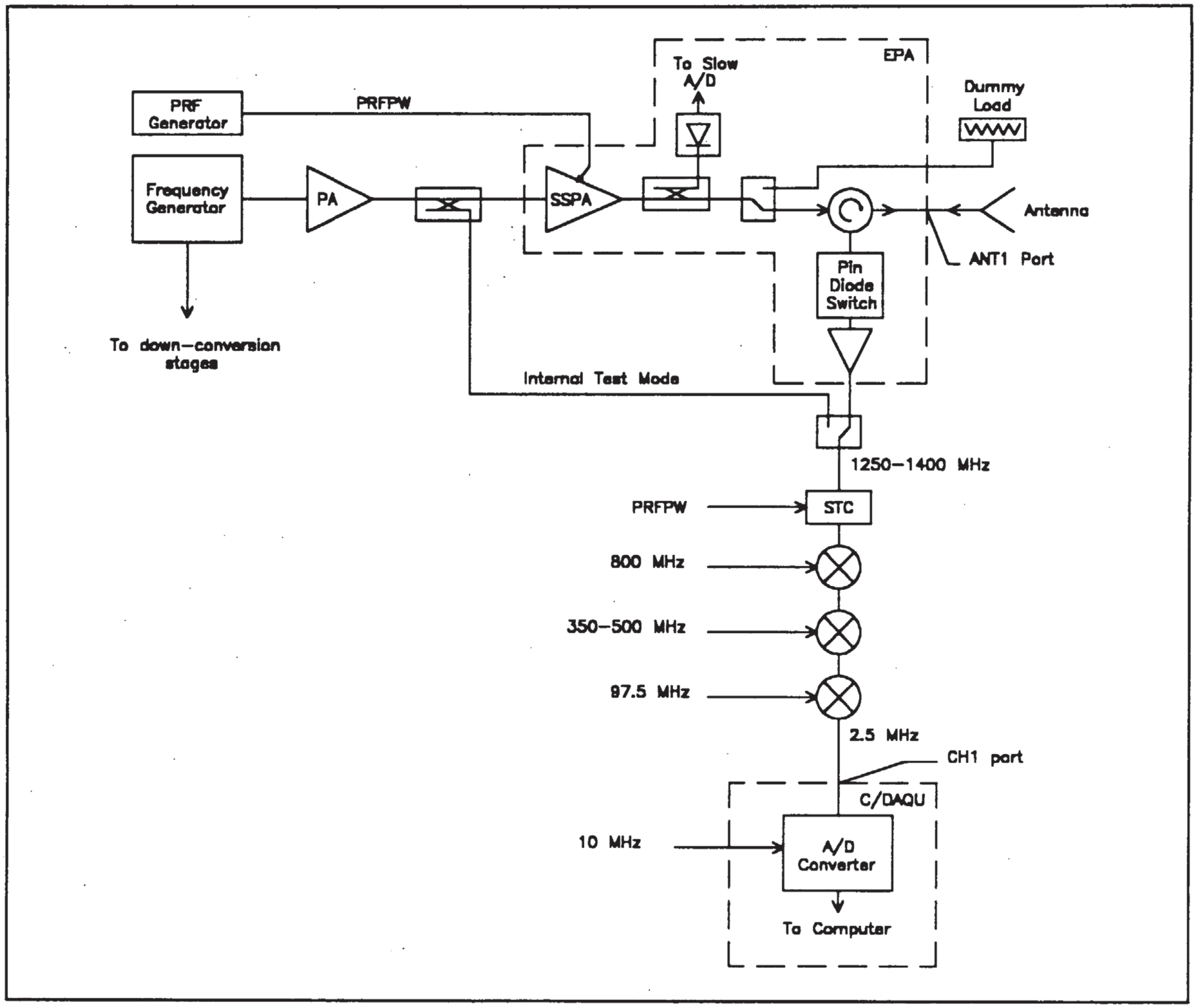

Figure 2 Simplified Functional Block Diagram of the Main Channel of the MAWS Transceiver

For each test described in this report, a specific command file was run to have the system exercise its range of capabilities.

When the system is operating, radar returns for each burst of pulses are collected on 8mm tapes. Upon completion of a run, the data can be extracted from the tapes to a PC. The collected data is separated during the extraction into binary files consisting of raw samples of the intermediate frequency (IF) signal, demodulated in-phase and quadrature (I and Q) data, and ARINC data. These can then be processed to give the desired information.

2.0 MAWS TRANSCEIVER TESTS

2.1 OUTPUT WAVEFORM

2.1.1 Objective. To verify the output power, frequency, harmonic levels, and intermodulation products of the radar transmitter. A secondary objective of this test is to verify and calibrate the operation of the task, referred to as the SLOWATOD task, which monitors the output power level.

2.1.2 Theoretical. The peak output power of the system as designed is 200 W. Average power depends on the programmed duty cycle, as shown in Table 1. Since average power is more easily and accurately measured than peak power, the average power will be measured, and the peak power will be inferred using the duty cycles shown in the table.

Table I: Theoretical Transceiver Average Power

PRF / PW combination	Duty Cycle	Theoretical Average Power
40 kHz, 1 μs	0.04	8 W
50 kHz, 1 μs	0.05	10 W
40 kHz, 3.3 μs	0.132	26.4 W
50 kHz, 3.3 μs	0.165	33 W

Measured frequencies should correspond to programmed values between 1250 - 1400 MHz (in 10 MHz increments). Since the frequency is derived from a 100 MHz crystal source with a precision of 14 Hz, the frequency accuracy should be high. The desired power level of the harmonics of the output signal is at least 70 dB below the fundamental. The solid state power amplifier (SSPA) is operating in class C mode, and hence is very nonlinear. Consequently, this should be the major source of harmonics.

Intermodulation products arise due to inherent nonlinearities in the mixers and amplifiers used in the frequency synthesizer portion of the design. These tones appear at the output of the devices at predictable frequencies, but at levels which are sometimes difficult to predict [1,2]. In narrowband designs, they can easily be eliminated using high Q, bandpass filters. However, when frequency agility is required, as it is in this case, the final filters in the transmit chain and the initial filters in the receive chain must pass the full operating bandwidth. Intermodulation products which lie in the band 1250 - 1400 MHz cannot be eliminated by these filters. The problem must be handled by careful selection of the intermediate frequencies and power levels at device inputs.

There are two major problems which occur when these tones are not eliminated. The first is that they may appear at frequencies which are not within the licensed band. This would be prohibited by Canadian frequency allocation licensing authorities. The second, more insidious problem is that these signals may be reflected by clutter targets into the receiver and passed through the receive chain, causing spurious detections. The desired specifications call for intermodulation products to be at least 70 dB below the fundamental.

The system is equipped with a Datel 8 bit, 2 MHz A/D card that is used solely to monitor the output power of the system. The SLOWATOD software task uses the A/D card to sample the peak power during a pulse, and raises a warning message if the power levels detected are outside the calibrated ranges allowed for each transmission frequency. The power level is recorded as an eight bit value on the 8 mm Exabyte tapes along with other parameters for each burst of pulses. The recorded value is measured using a diode detector, and varies as the square root of power. Since these values are the only record of transmitted power levels during the flight trials, it is necessary to calibrate them by comparison to measured output power levels in the laboratory.

2.1.3 Procedures. Average power output was measured by connecting a 50 Ω load to the antenna output port, designated ANT1, on the EPA, and coupling off a small portion of the transmitted signal using a precision 20 dB directional coupler. The coupled signal was attenuated by 30 dB to bring the RF levels within the operating range of the power meter. Peak power was then calculated using the duty cycle of the pulse, as measured on a LeCroy 9450 digital oscilloscope.

A second method of collecting power measurements was then used to confirm the readings obtained in the test described above. Peak power was measured directly using the same basic set-up, but replacing the power meter with a crystal detector. The output of the detector was connected to the digital oscilloscope. The timebase and trigger were adjusted to display one complete pulse and the peak voltage output was read directly off the CRT. The detector was calibrated against a known RF source and the voltage readings equated to RF peak power.

Once the power measurements were taken, data was extracted from the tape to calibrate the slow A/D by comparing the 8 bit recorded values to the absolute power levels.

Both the harmonic and the intermodulation product levels relative to the fundamental component of the signal were measured directly, using a Hewlett Packard 8566B spectrum analyzer connected to the ANT1 antenna port. Harmonic and intermodulation product power levels were then computed using the results from the first part of the procedure. The output frequency was read directly off the spectrum analyzer as well.

2.1.4 Results. Analysis of the output spectrum showed that the output frequency was equal to the programmed frequency within the calibration tolerance of the spectrum analyzer, which is $\pm$ 0.1%.

The peak power levels shown in Table II were calculated from average power levels measured after a system warmup time of approximately 50 minutes. It can be seen from Table II that peak power levels after system warmup are above the specified 200 W peak in all cases except for the higher duty cycle waveform at 1250 MHz. The highest recorded peak power level is actually 325.3 W, which is well over the required level. These readings were confirmed using the second power measurement method described in 2.1.3.

One problem that was discovered, however, is that when the system is initially turned on, the output pulse shape of the solid state power amplifier (SSPA) is distorted at 1290 and 1300 MHz for the highest duty cycle, i.e. 50 kHz PRF with a 3.3 μs pulse width. The inverted detected output for a 50 kHz PRF and 3.3 μs pulse is shown in Figure 3 when the system is cold. The figure shows that there is a power drop in the middle of the pulse. As the system warms up, the pulse gradually returns to its normal rectangular shape. This takes approximately 50 minutes.

Table II: Measured Peak Power Values

Freq (MHz)	Peak Power (W) 40 kHz PRF, 1 μs pulse	Peak Power (W) 40 kHz PRF, 3.3 μs pulse	Peak Power (W) 50 kHz PRF, 1 μs pulse	Peak Power (W) 50 kHz PRF, 3.3 μs pulse
1250	213.0	302.9	196.6	192.4
1260	265.4	262.1	224.0	214.9
1270	284.7	281.5	238.5	229.4
1280	303.3	301.0	253.8	243.4
1290	305.7	301.0	264.4	253.7
1300	305.7	302.9	272.8	261.6
1310	318.0	314.6	282.7	270.1
1320	325.3	320.4	287.3	274.9
1330	325.3	320.4	288.8	276.8
1340	318.0	314.6	283.5	272.5
1350	308.2	304.8	276.6	267.1
1360	291.1	289.3	266.0	258.0
1370	278.8	275.7	253.0	247.0
1380	256.8	252.4	235.5	230.6
1390	230.1	227.2	209.6	205.8
1400	237.5	234.9	217.9	213.6

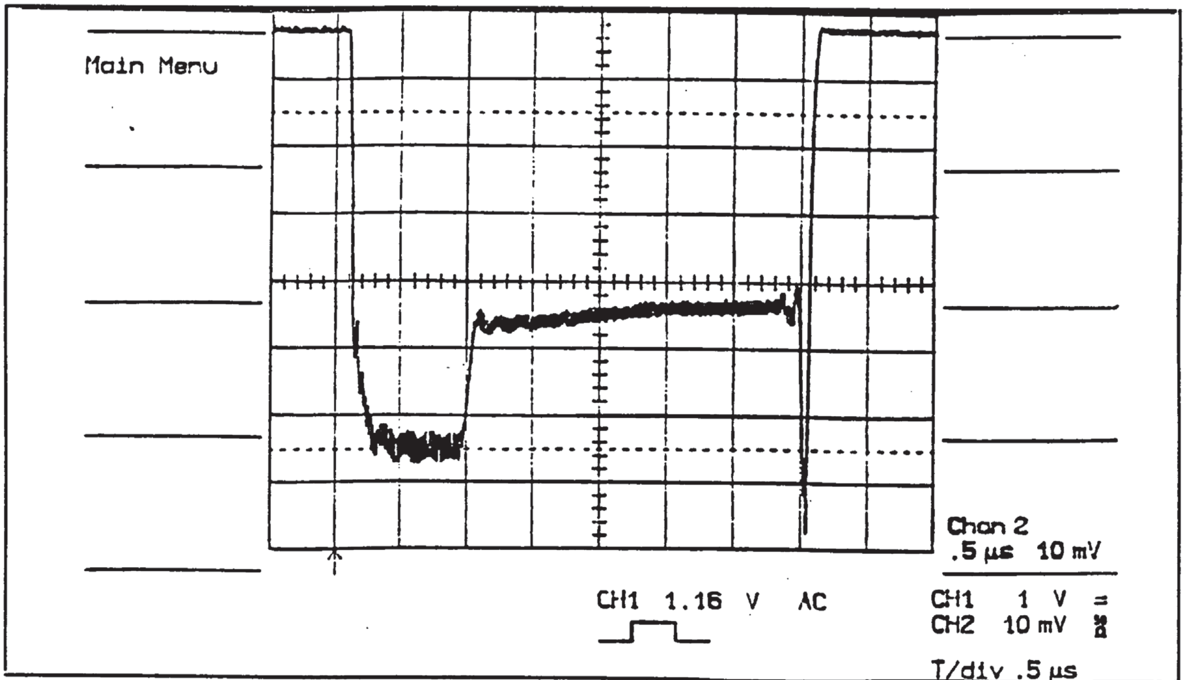

Figure 3 Pulse Distortion Problem

The voltage levels in the distorted region of the pulse were measured and converted to power readings using the crystal detector and oscilloscope setup described in Section 2.1.3. The peak power readings for 1290 and 1300 MHz when the system was cold were only 87.9 W and 99.4 W respectively, well below the specified 200 W. This power dropout was not recorded for any other frequency, and did not occur at any of the lower duty cycles. This will have ramifications for the flight trials, as the system may not have 50 minutes to warm up before the trials occur. Consequently, these frequencies may have to be avoided altogether, or noted in the collected data as potential anomalies.

The power level at the input to the SSPA was investigated because of the significant increase in the output power level at some frequencies compared to the specified 200 W (53 dBm). The manufacturer of the SSPA had specified a peak power input level of 0 dBm, and an input overdrive protection at +8 dBm. The signal input to the SSPA was monitored under normal operating conditions, and it was found that the transceiver itself drives the SSPA at anywhere from +2 to +5 dBm. This input level changes with frequency, and the transceiver produces the highest input levels (i.e. approximately 5 dBm) near the middle of the frequency range. This explains the higher output power levels seen in this region.

The input to the SSPA was then replaced with a frequency synthesizer, which allowed the input level to be adjusted. It was discovered that the SSPA requires a minimum input of 0 dBm to provide any output power. A higher input level to the SSPA produces a higher output at any frequency. With the level set at +2 dBm, no pulse distortion was seen at any frequency even when the system was cold. Thus the SSPA is being overdriven according to the manufacturer's specifications at all frequencies just to provide an output, but apparently cannot handle a +5 dBm input at the higher duty cycle when it is cold.

Ideally, the MAWS output power should remain constant. One possible "quick fix" solution to combat the problem would be to add a variable attenuator that would adjust the input to the SSPA to a more desirable level on a frequency by frequency basis. No remedy has been attempted at this point by DREO.

The harmonic levels were measured for the 40 kHz PRF and both the 1 μs and 3.3 μs pulse widths, and are displayed in Table III. The worst case harmonic is a third harmonic at 1290 MHz which is only 43 dB down from the fundamental.

Some of the more substantial IM products measured at the output of the antenna port are displayed in Table IV. Only IM products above -48 dBc are included in this table. Based on the intermodulation products seen in the output, the cleanest frequencies are 1350 MHz, 1390 MHz, and 1400 MHz.

Table III: Measured Harmonic Levels

	1 μs Pulse		3.3 μs Pulse	
Freq (MHz)	2nd harmonic level (dBc/dBm)	3rd harmonic level (dBc/dBm)	2nd harmonic level (dBc/dBm)	3rd harmonic level (dBc/dBm)
1250	-53/0	-48/5	-55/0	-49/6
1260	-53/1	-48/6	-55/-1	-48/7
1270	-53/2	-47/8	-59/-5	-50/4
1280	-55/0	-45/10	-59/-4	-47/8
1290	-59/-4	-43/12	-62/-7	-43/12
1300	-59/-4	-44/11	-63/-8	-44/11
1310	-59/-4	-45/10	-64/-9	-44/11
1320	-59/-4	-46/9	-65/-10	-46/9
1330	-59/-4	-51/4	-64/-9	-51/4
1340	-58/-3	-58/-3	-64/-9	-60/-5
1350	-58/-3	-55/0	-66/-11	-57/-2
1360	-58/-3	-54/1	-66/-11	-56/-1
1370	-58/-4	-51/3	-65/-11	-53/1
1380	-58/-4	-50/4	-61/-7	-51/4
1390	-58/-4	-53/1	-59/-5	-51/3
1400	-57/-3	-53/1	-58/-4	-53/1

Table IV: Intermodulation Product Frequencies and Levels

Fund. Freq (MHz)	IM freq (MHz) / level (dBc)	IM freq (MHz) / level (dBc)	IM freq (MHz) / level (dBc)	IM freq (MHz) / level (dBc)	IM freq (MHz) / level (dBc)
1250	1380/-29	1400/-29	1510/-33	1530/-43	
1260	1440/-43				
1270	1340/-42	1350/-41			
1280	1340/-40	1360/-39	1380/-40		
1290	1350/-41	1360/-41	1370/-35	1380/-42	1410/-36
1300	1400/-25				
1310	1390/-22	1470/-43			
1320	1380/-30	1440/-32			
1330	1370/-27	1410/-24			
1340	1360/-25	1380/-22	1400/-42		
1350	1400/-47				
1360	1380/-32	1400/-26			
1370	1410/-31	1450/-36			
1380	1440/-39	1500/-48			
1390					
1400					

The values recorded from the SLOWATOD task were compared with the measured peak power levels to provide a calibration curve. The results are tabulated in Table V, and plotted on a calibration curve in Figure 4. The recorded value varies as the square root of the power, so a plot of the measured power level in Watts vs. the (recorded value)^2 should produce a linear relationship. We can use the relationship $P = kA^2$ where P is the power in Watts, A is the recorded value and k is the slope of the graph to determine the actual power levels transmitted during the flight trials. Based on the curve, the value of k is approximately 0.00825. This value should provide calibrated power measurements which are accurate to within about one dBm. This is more than sufficient for its purpose.

Table V: Calibration Data for SLOWATOD Values

Freq (MHz)	Measured Power Level (dBm)	Measured Power Level (W)	SLOWATOD record on tape
1250	54.4	275	191
1260	54.4	275	193
1270	54.6	288	194
1280	54.8	302	196
1290	54.9	309	197
1300	54.7	295	198
1310	55.0	316	197
1320	55.1	324	196
1330	55.0	316	194
1340	54.9	309	190
1350	54.8	302	186
1360	54.0	251	182
1370	53.6	229	178
1380	53.1	204	168
1390	53.3	214	158
1400	52.8	191	155

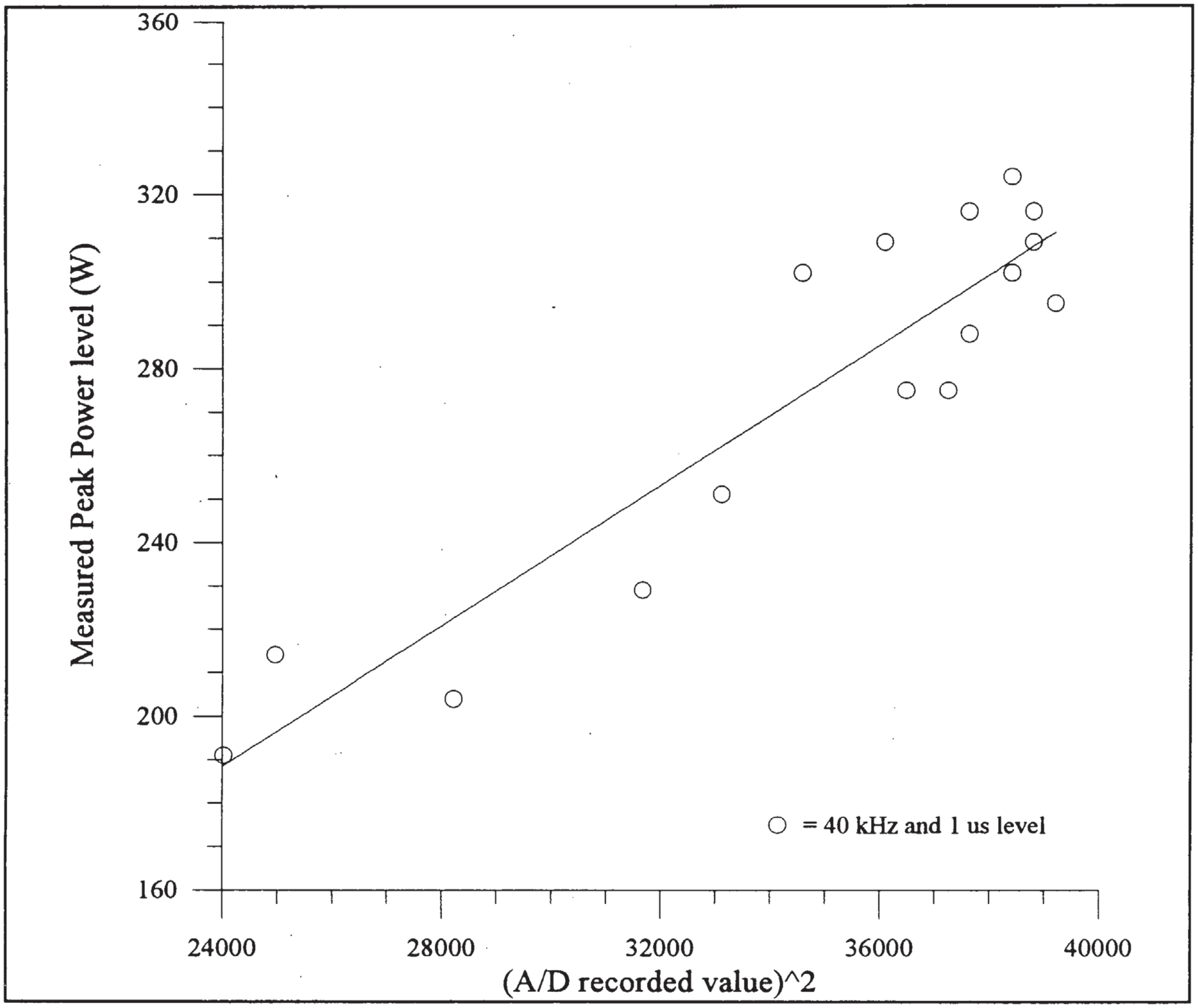

Figure 4 Calibration Curve for SLOWATOD Recorded Values

2.2 GAIN AND NOISE FIGURE OF RECEIVE CHAIN

2.2.1 Objective. To measure the gain and noise figure of each receive chain.

2.2.2 Theoretical. The noise figure of a radar is the ratio of the noise measured at the output of the receive chain to the fundamental thermal noise (amplified by the receiver gain) that is associated with the input impedance of the receive chain as seen at the antenna ports on the EPA. Detection performance of the MAWS transceiver is ultimately limited by the output noise power. Consequently, it is desirable to have the noise figure as close to unity as possible to maximize the target detection range.

The system gain merely scales the received signal in such a way as to maximize the dynamic range of the digitized signal. The gain should, therefore, be constant from frequency to frequency, set low enough so as to saturate the A/D converter only infrequently when a strong clutter signal is present, and set high enough that, in the presence of noise only, the signal varies by a substantial number of bits. This latter requirement minimizes the effect of quantization noise on system performance.

The MAWS transceiver has two receive chains: one for a main channel and one for a guard channel. The desired noise figure for the receive chain for the main channel (channel 1) is $\leq$ 3 dB. The guard channel (channel 2) is identical except that it does not have a pin diode switch for isolation, and thus should have a lower noise figure. No gain specifications were set, but the gain of each receive chain was designed to be approximately 70 dB.

2.2.3 Procedures. For the gain and noise figure measurements, the SSPA was fed directly into a dummy load (see Figure 2) to eliminate all but the receiver's contribution to the noise figure. The noise figure measurements were taken by injecting a known calibrated noise source into the antenna ports and measuring the output noise figure directly with a Hewlett Packard 8970A noise figure meter. Ideally, both gain and noise figure measurements would be taken at the very end of the receive chain to include the contribution of all components. The noise figure measurements, however, were taken at an earlier stage in the receive chain at the output of the EPA (1.25 - 1.40 GHz), as the meter was not capable of functioning at the last intermediate frequency (2.5 MHz). This should not affect the accuracy of the results, as the major noise contribution occurs at the first amplification stage, which is inside the EPA.

Gain measurements were taken in a similar manner. A calibrated RF source was substituted for the noise source, and the output power level at the last IF (2.5 MHz) was measured. The ratio of the output to the input power represents system gain.

2.2.4 Results. As shown in Table VI, the worst case EPA noise figure for channel 1 and channel 2 is 2.56 dB and 1.51 dB respectively.

As mentioned earlier, for systems with high gain such as this one, the overall system

Table VI: Gain and Noise Figures for the Two Receive Channels

Freq (MHz)	Gain (dB) CH1	Noise Figure (dB) CH1	Gain (dB) CH2	Noise Figure (dB) CH2
1250	79.4	2.31	86.6	1.51
1260	78.4	2.38	87.5	1.50
1270	78.4	2.41	87.3	1.51
1280	77.9	2.44	87.5	1.51
1290	75.5	2.49	87.5	1.50
1300	76.7	2.52	86.6	1.49
1310	77.3	2.54	86.9	1.50
1320	78.9	2.56	86.9	1.50
1330	79.2	2.53	84.5	1.49
1340	78.7	2.51	85.1	1.50
1350	78.7	2.50	85.7	1.50
1360	78.5	2.47	85.7	1.50
1370	75.8	2.45	85.7	1.50
1380	75.8	2.43	85.7	1.49
1390	75.8	2.42	84.5	1.49
1400	76.2	2.44	83.8	1.49

noise figure is determined by the input stages of the receiver. The reason is not that these stages are inherently more noisy than others but that, amplified by the receiver's full gain, noise generated in the initial stages swamps out the noise generated farther along. Consequently, although the output that has been measured in this test occurs after the first amplification stage, it can be assumed that the overall noise figure specification of 3 dB is met by the system.

For channel 1, the gain varies from 75.5 dB to 79.4 dB across the band, a difference of

3.9 dB. For channel 2, the gain varies from 83.8 dB to 87.5 dB.

The noise power relative to the quantization noise power contributed by the A/D converter can be computed. The thermal noise power for an ideal receiver [3] is:

$$\textit{Mean noise power} = kT_oB, \tag{2-1}$$

where k is Boltzmann's constant, T is the temperature in degrees Kelvin, and B is the single sided system bandwidth. At room temperature, for a receive channel bandwidth of 2 MHz, this background noise power is:

$$\begin{aligned} kT_oB &= (1.38x10^{-23}\ \textit{watt-second}/°K)\ (290°K)\ (2x10^{6}\ Hz) \\ &= 8.0x10^{-15}\ \textit{watts} \\ &= -111\ dBm. \end{aligned} \tag{2-2}$$

For the transceiver receive chain, this noise is increased by approximately 3 dB as indicated by the measured noise figure. With a gain of between 75.5 dB and 79.4 dB, the total noise power seen at the A/D converter varies between -32.5 dBm and -28.6 dBm. Because $P=V^2/R$, this equates to a voltage standard deviation of between 5.30 x 10^{-3} V and 8.31 x 10^{-3} V in the 50 Ω system. Full scale deflection on the A/D boards occurs at ±1 V. Since a 12 bit A/D board is used, the 2 V input range is represented by 2^{12} or 4096 quantization levels. Hence, the thermal noise standard deviation, measured in quantization levels, varies from 11 to 17 levels (4 to 5 bits). Since it has a Gaussian distribution, it can be represented using five bits (excluding the sign bit) 65 % of the time, and six bits 94 % of the time.

The quantization noise standard deviation, on the other hand, has a value of 1/sqrt(12) when measured in quantization levels [3]. Thus, the quantization noise power is more than 30 dB lower than the thermal noise power. Quantization noise can therefore be disregarded in system performance calculations. In the design of the receive chain, an appropriate value for the system gain is one for which the thermal noise is 15 to 20 dB higher than the quantization noise. Thus, in the MAWS, the system gain could probably be 10-15 dB lower, with the attendant dynamic range improvement, and still provide acceptably small quantization noise levels.

The clutter power at the receive chain output will depend on the profile that the aircraft flies. For a low level flight, clutter power may be on the order of 55 dB larger than the noise power in the near range gates. Assuming the clutter power is exponentially distributed, and following the same procedure, the voltage standard deviation would be between 2.98 V and 4.67 V at the A/D input. Thus, in a flight scenario such as the one described above, the near range gates would be saturated without any added protection. The MAWS has a sensitivity time control (STC) which is designed to vary the sensitivity of the receive chain. The STC can provide up to 31.1 dB of attenuation for the close-in targets and clutter, bringing the returns within the dynamic range of the A/D converter.

2.3 SINGLE TONE TEST

2.3.1 Objective. To measure the overall receiver image rejection, spurious content, and noise.

2.3.2 Theoretical. When ideal complex demodulation of a Doppler shifted IF tone is performed, a Fast Fourier Transform (FFT) analysis of the resulting baseband signal yields only a component at the appropriate Doppler frequency. For practical complex demodulation schemes, an FFT analysis of the baseband signal would show an additional component at the negative of that Doppler frequency. The receiver image rejection is a measure of the degree to which this image component is attenuated in magnitude relative to the desired component.

The C/DAQU signal processing is required to perform a complex demodulation of the IF signal so that, upon FFT analysis, the image frequency components will be suppressed by more than 70 dB relative to the desired signal components. Furthermore, the receive chain should be free of spurious signals and nonlinearities such that all discrete components of the digital spectrum are suppressed more than 70 dB below the desired signal. The exception to this is that a DC component, due to an A/D bias, is acceptable.

The image frequency component of the signal is attenuated in the MAWS system by the use of a digital demodulation scheme [8]. This method is implemented by sampling the received signal at an intermediate frequency (IF), and performing the final complex demodulation digitally. This obviates the need for precise amplitude and phase balance in the I and Q channels. The attenuation of the unwanted image is then a digital signal processing task. The digital filter used should provide 140 dB of suppression of the unwanted image.

The expected signal-to-noise ratio (SNR) for a full-scale signal tone at the A/D can be computed using the noise power results from Section 2.2. For the frequencies with the highest receiver gain, the noise standard deviation σ is 17 quantization levels, so the noise power, in terms of quantization levels, is proportional to σ^2 or $17^2 = 289$. For a full-scale signal on the A/D board, the signal amplitude A, in quantization levels, is approximately 2048. Output power for a single-frequency tone is proportional to $A^2/2$, and in quantization levels, this is $2048^2/2 = 2.1 \times 10^6$. Thus, the input signal to noise ratio is:

$$\begin{aligned} Input\ SNR &= 10 x \log\left(\frac{2.1x10^6}{289}\right) \\ &= 38.4 dB. \end{aligned} \tag{2-3}$$

If the signal is weighted with a Hamming window prior to performing an FFT, this degrades the output SNR by between 1.23 dB and 3.0 dB. Finally, the coherent integration associated with performing an FFT on 1024 samples improves the SNR by 10log(1024) = 30.1 dB, so the final SNR should be approximately 65 dB.

2.3.3. Procedures. The SSPA output was disconnected from the antenna port and connected to a dummy load, as indicated in Figure 2. An HP 8660C signal generator which provided an output sine wave with an offset of 13 kHz from the transmitted frequency was connected to the port ANT1. This signal simulated a Doppler shifted return from a target with a closing velocity of:

$$\begin{aligned} \dot{R} &= \frac{f_d c}{2f} \\ &= \frac{(13x10^3 s^{-1})(3x10^8 m/s)}{2(1250x10^6 s^{-1})} \\ &= 1560 m/s \end{aligned} \tag{2-4}$$

or Mach 4.6. The input level to the A/D converters was monitored (at CH1 port in Figure 2), and the level of the sine wave was adjusted to bring the A/D input as close to its maximum of ± 1 V peak as possible. The appropriate command file was run, and 1024 complex samples were collected. These samples were weighted with a Hamming window and an FFT was performed. The amplitude of the result was then displayed in decibels below the fundamental for analysis. This procedure was repeated for each of the 16 possible transmission frequencies.

2.3.4 Results. In the current implementation, once the signal is digitally demodulated to baseband, the first eight samples from each range gate are passed through a digital finite impulse response (FIR) filter with a bandwidth of 2 MHz. As a result of the digital filtering process, one value from each range gate for each pulse is kept, effectively lowering the sampling rate to one sample per pulse for each range gate. For a 40 kHz PRF this means a sampling rate of 40 kHz. With a receiver bandwidth of approximately 2 MHz and a final sampling rate of 40 kHz, the spectrum is heavily aliased. The resultant spectrum at a frequency of 1400 MHz for range gate 5, in conjunction with a 40 kHz sampling rate, is shown in Figure 5.

In Figure 5, a spectral component appearing at f kHz is the complex summation of components at (f + 40i) kHz where i takes on integer values from -25 to 25. Naturally, all spurious signals and noise in the range -1 MHz to 1 MHz will be aliased into this spectrum. The signal is clearly visible at 13 kHz. The sharpness of the signal spike indicates that the synthesized signal has good close-in phase noise.

There are also a number of other significant features of this graph. The noise floor is very close to that predicted by theory; a SNR of 65 dB was expected for this type of input, and the noise floor is roughly 60 to 65 dB down from the fundamental. The digital filter used in the design has more than 140 dB image suppression, so the image is buried in the noise floor as expected. The noise seems to exhibit a periodic quality, and is slightly higher around 0 kHz in each of the spectra. The reason for this is not yet known.

The spectrum for the 1400 MHz single tone test is a typical case in terms of image

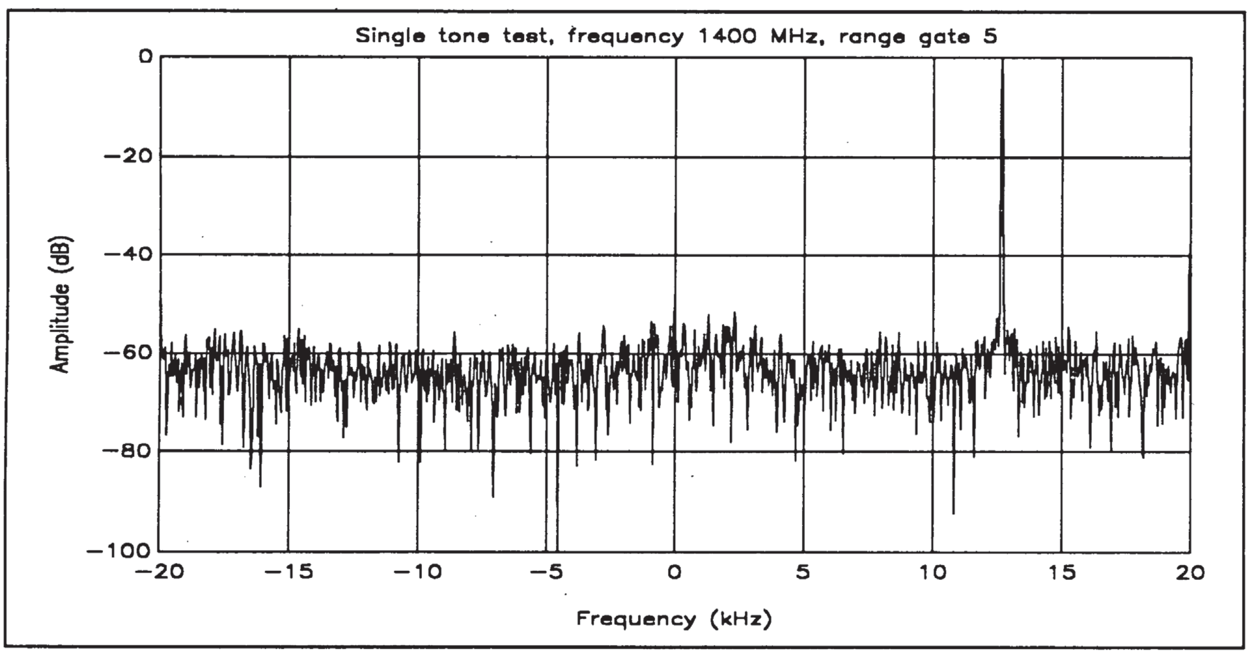

Figure 5 Single Tone Test Sample Results

suppression and noise floor level. The spectrum for the 15 other transmission frequencies can be found in Appendix A. These results confirm the noise figure measurements taken in Section 2.2.

2.4 TWO TONE TEST

2.4.1 Objective. To measure the intermodulation products of the IF amplifiers and mixers.

2.4.2 Theoretical. A major problem of high dynamic range systems is that for a signal with bandwidth, its multiple spectral components will be mixed together as a result of nonlinearities in the receive chain. The major effect of this intermodulation (IM) is to spread the spectrum of the signal. A convenient measurement of these intermodulation products can be done with just two tones. If two relatively closely spaced tones at f_1 and f_2 are combined and added to the input of a nonlinear system, the output spectrum in general will have IM products at $mf_1 \pm nf_2$ where m and n are integers. The levels of these signals generally diminish as m and n increase, and only a certain number of them will fall within the system bandwidth after demodulation to baseband. For the MAWS transceiver, only IM products at frequencies $(mf_1 - nf_2)$ and $(mf_2 - nf_1)$ where $m,n>0$ and $(m-n)=1$ fall within the system bandwidth. The desired specifications for the system call for IM products within the system bandwidth to be suppressed by 70 dB relative to the fundamental components for input signals near the maximum range of the A/D converters.

2.4.3 Procedures. The SSPA output was connected to a dummy load. A two tone input was supplied by two separate sources: a Marconi Instruments 2041 signal generator and an HP 8660C signal generator. These RF sources were offset in frequency by 7 kHz and 13 kHz from the carrier, combined, and applied to the receiver front end. As in Section 2.4.2, the output levels were adjusted until the input to the A/D converters was near its maximum value (± 1 V peak). At each transmitted frequency, 1024 complex samples were collected, weighted with a Hamming window, and an FFT performed. The amplitude of the result was displayed in decibels below the fundamental for analysis.

2.4.4 Results. The resultant spectrum at range gate 5 for an input of 1260 MHz and a sampling rate of 40 kHz is shown in Figure 6. A spectral analysis for the other transmission frequencies can be found in Appendix B. The $2f_1$-f_2 and $2f_2$-f_1 tones at 1 kHz and 19 kHz respectively are only about 38 dB below the desired signals. Also, there are other large spurious signals at -10 kHz, 10 kHz, and 20 kHz, which do not seem to relate to the two inputs. It is possible that the signals appearing at ± 10 kHz are due to some sort of baseband amplitude modulation. The noise floor in general is somewhat higher than that seen in the single tone test.

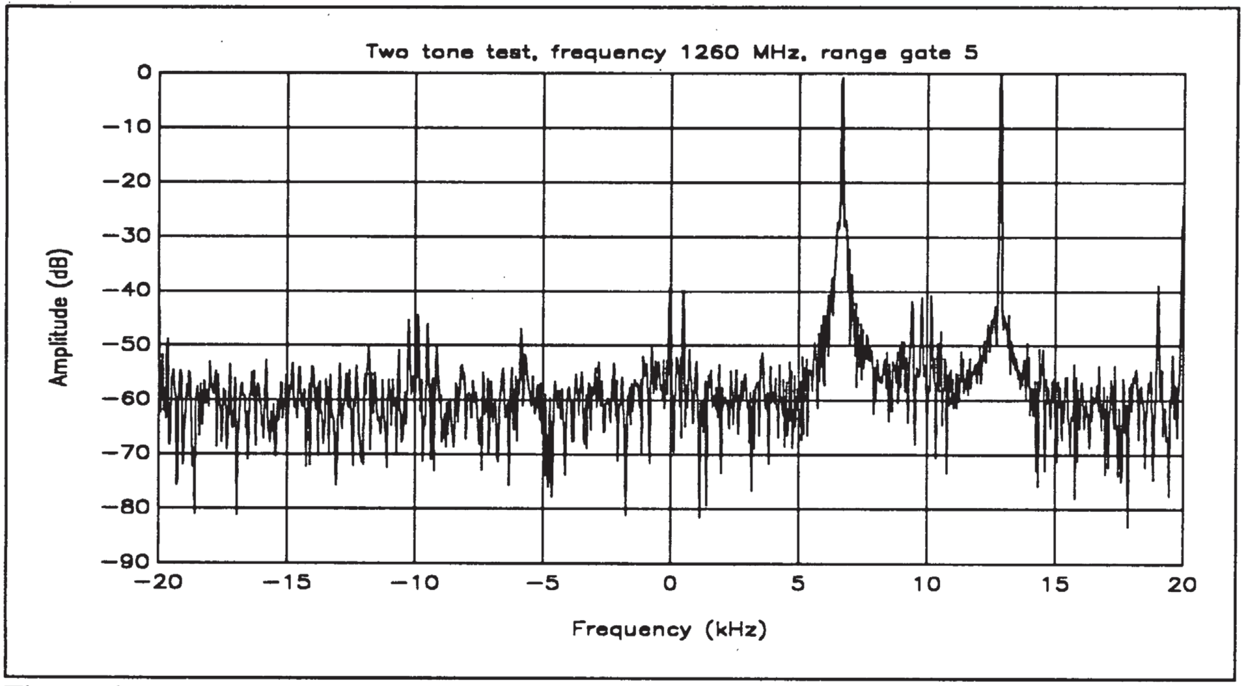

Figure 6 Two Tone Test Sample Results

2.5 FREQUENCY RESPONSE OF RECEIVE CHAIN

2.5.1 Objective. To measure the frequency response of the receive chain.

2.5.2 Theoretical. In Sections 2.3 and 2.4, the response of the receive chain to a narrowband signal was tested. While these are adequate tests to measure a desired channel characteristic, in operation the signal will consist of the summation of a large number of wideband signals, with bandwidths of up to 2 MHz. If the frequency response of the receive chain is uneven over the system bandwidth, excessive ringing will occur, thereby smearing return echoes over a number of range gates and reducing range resolution. There will also be a SNR penalty, as the receiver will no longer be properly matched to the signal. For these reasons, it is desirable that both receive channels exhibit flat response within ± 1 MHz of the centre frequency. A simple means of testing this is to introduce a white noise source at the antenna input. Spectral analysis at the 2.5 MHz IF output should show a flat spectrum over this band, with less than a 1 dB variation in response across this band.

2.5.3 Procedures. To measure the frequency response of the receive chain, an HP Model 346B white noise generator was connected to the input of each of the antenna ports. The output at the last IF was monitored with a spectrum analyzer. The analyzer was adjusted to cover the appropriate bandwidth, and the flatness was measured directly from the CRT.

2.5.4 Results. The spectrum showed a maximum of 1.5 dB variation across the band for all frequencies between 1250 MHz and 1400 MHz, which is adequate.

2.6 A/D TIMING VERIFICATION

2.6.1. Objective. To verify the timing of the A/D sampling.

2.6.2. Theoretical. According to the system specifications, the A/D sampling is turned off during the nominal period of pulse transmission, and, following the end of pulse transmission, is switched back on at the earliest point in time that a return signal is expected to arrive at the A/D converters. This turn-on time should be sufficiently delayed to account for any signal delays in the receive chain caused by the presence of analog filters.

2.6.3. Procedures. The timing of the trigger signal that turns on the A/D converters was first measured relative to the pulse transmission. This was done by monitoring the A/D trigger signal on the oscilloscope, along with a sample of the transmitted signal obtained with a 20 dB coupler in the signal path from the ANT1 port to a 50 Ω dummy load. The signal delay in the receive chain was then measured by observing on the oscilloscope the time skew between the transmitted pulse, coupled off at the ANT1 port, and the associated pulse, leaked through the pin diode switch and circulator, that appears at the input to the A/D converter.

2.6.4. Results. The relative timing of the A/D trigger and the transmitted pulse is shown in Figure 7. The Curve A trace is the transmitted pulse, inverted on the oscilloscope display, and the Curve B trace is the A/D trigger signal. It is clear from this figure that the A/D converter is prematurely starting to sample before the end of pulse transmission, by an amount of time indicated by the marker separation. The marker separation is about 300 ns. The trigger signal itself is fairly noisy, which is not desirable.

In Figure 8, the signal delay through the receive chain is shown. The lower trace in this

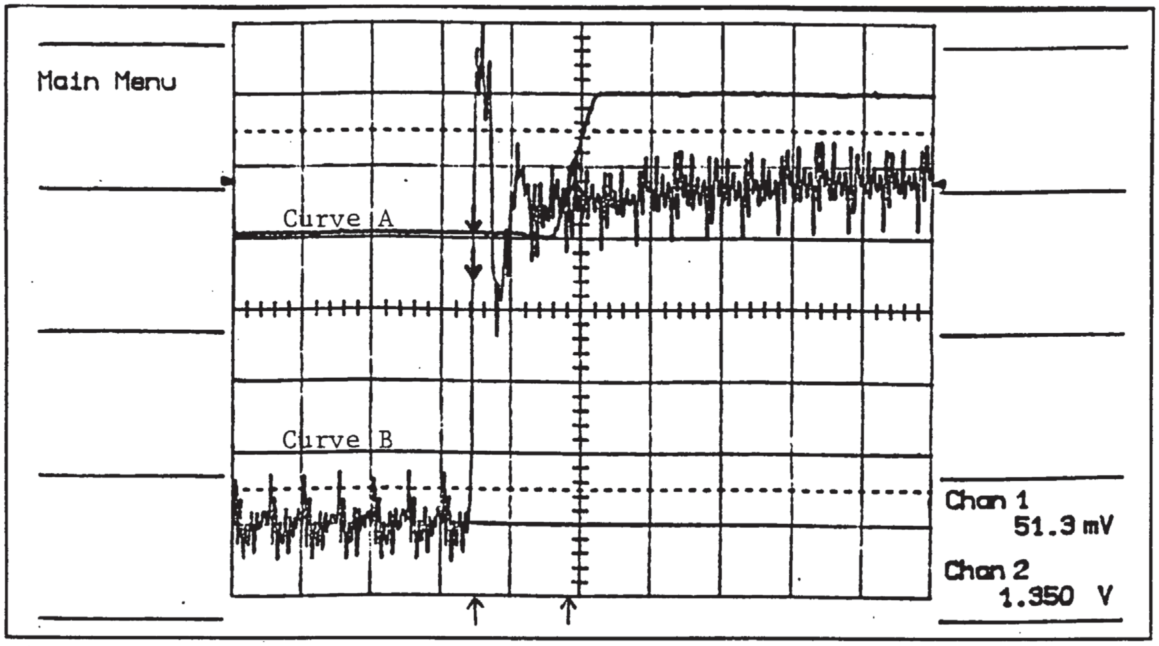

Figure 7 Relative Timing of A/D Trigger and Transmitted Pulse

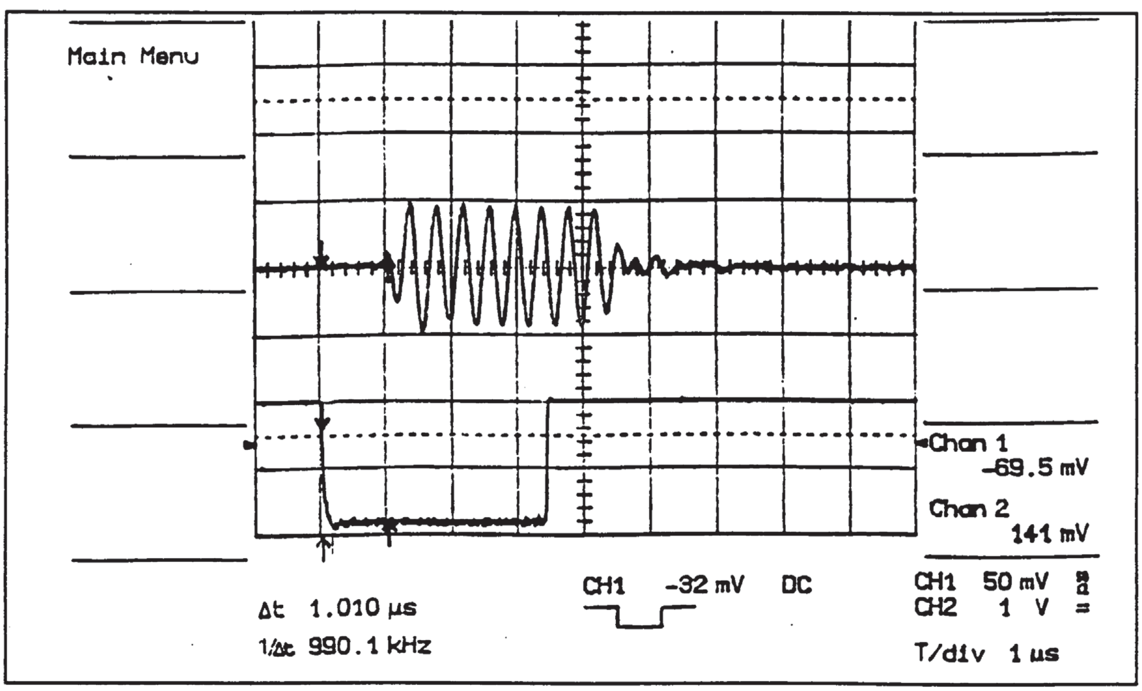

Figure 8 Delay of Signal through Receive Chain

figure is the inverted envelope of the transmitted pulse, monitored at the ANT1 port, and the upper trace is the leaked pulse measured at the input to the A/D converter. This figure indicates that there is a 1 microsecond signal delay in the receive chain.

These measurements suggest that for the A/D converters to operate as intended, the timing of the A/D trigger signal should be changed so that the A/D converters start sampling 1.3 microseconds later than is currently the case, or in other words, 1 microsecond after the end of the pulse transmission.

3.0 DREO ENHANCEMENTS TO SYSTEM HARDWARE

3.1 2.5 MHz FEEDTHROUGH SWITCH

In normal operation, the Solid State Power Amplifier (SSPA) is pulsed with a control signal that essentially turns it on and off with the programmed pulse length at the pulse repetition frequency. During testing of the transceiver, it was observed that a residual signal component at the last IF frequency appears in the raw digital data during the interpulse period. This implied that when the SSPA is turned off, it still generates a small RF signal that leaks through the receive chain. This is a concern, for this may decrease the dynamic range of the system.

To attempt to remedy the situation, a Minicircuits AYSWA-2-50DR switch was added before the SSPA to provide even more isolation of the RF signal input. The switch is controlled with the same control signal that pulses the SSPA. The switch, then, closes during a pulse and allows the RF to feed through, and goes off (to a termination) between pulses to provide 30 dB of extra isolation. Raw A/D data shown in Figure 9 was collected with and without the switch

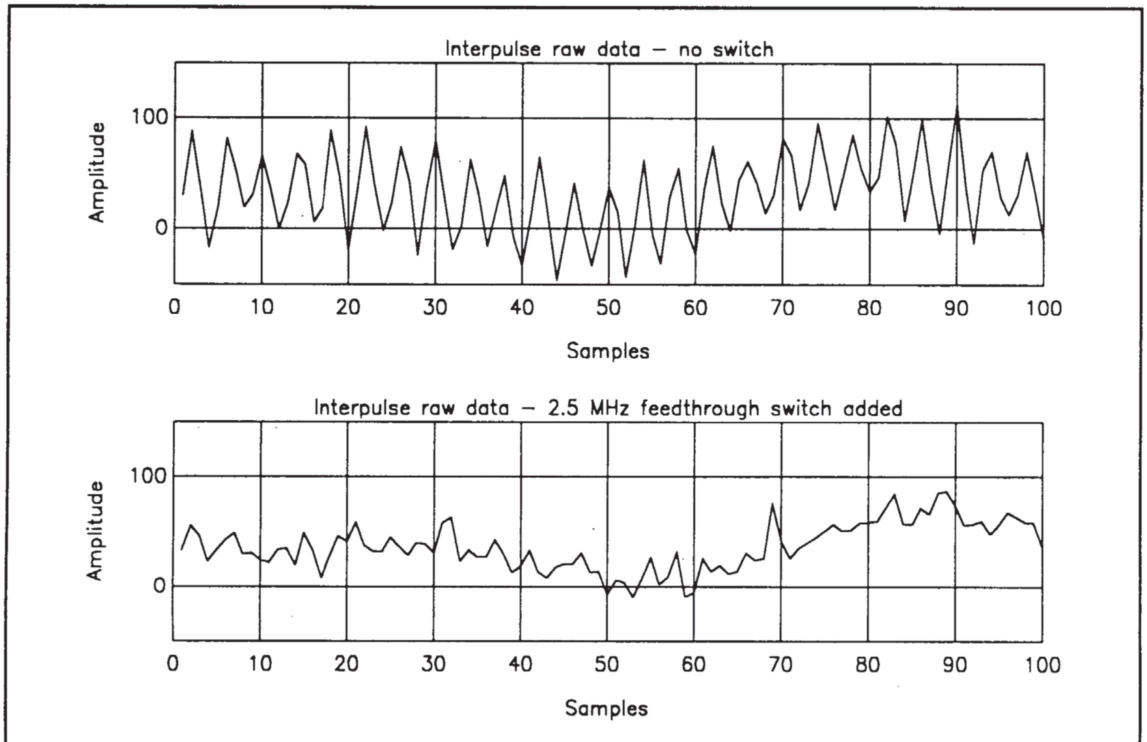

Figure 9 Implementation of 2.5 MHz Feedthrough Switch - Raw Data

implemented .

Spectral analysis of this data with a single tone input is shown in Figure 10. The Figure indicates that the switch has decreased the 2.5 MHz feedthrough by approximately 30 dB, as expected.

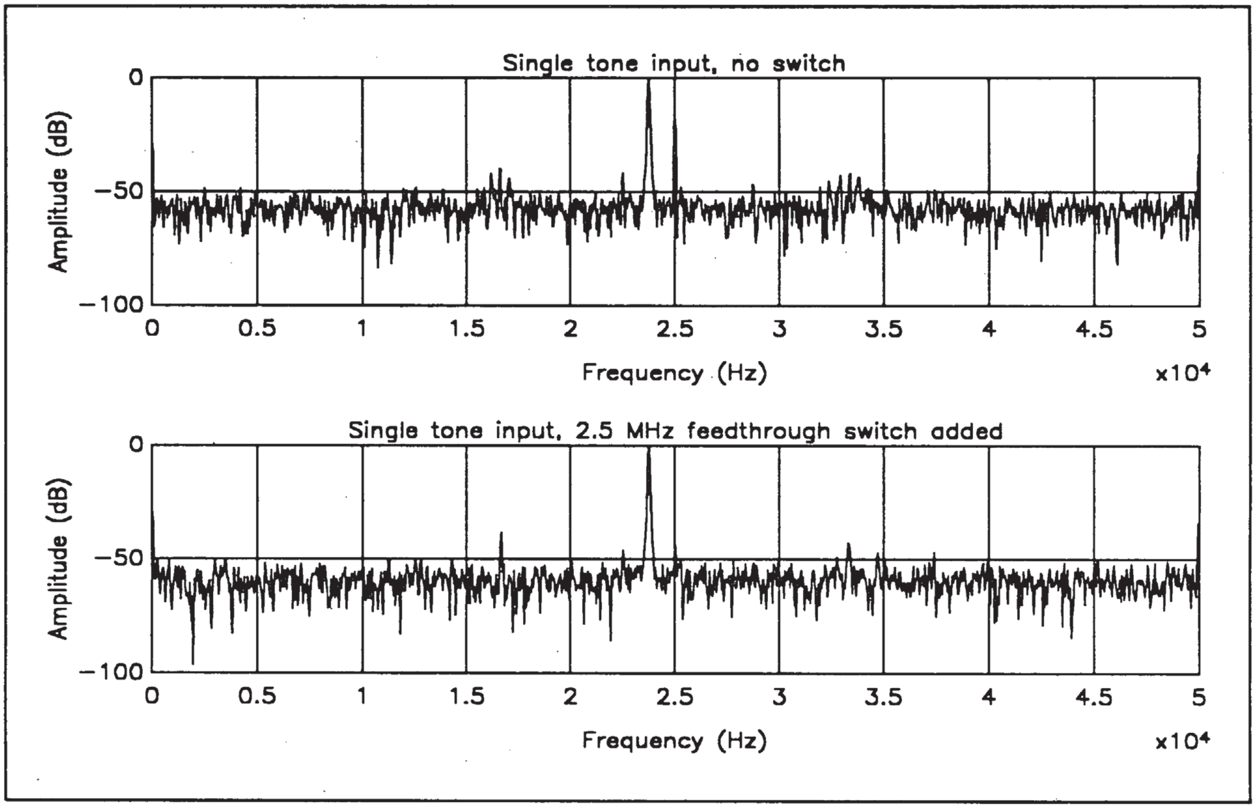

Figure 10 Implementation of 2.5 MHz Feedthrough Switch - Spectral Analysis

3.2 SYSTEM POWERUP PROTECTION SWITCH

During normal operation, the SSPA is pulsed only when a GO command occurs in the command file to transmit a burst. During initial powerup, however, it was discovered that the MAWS transmits with a 3.3 μs pulse width and a 50 kHz PRF. The system ceases transmission and returns to a known state later in the initialization procedure when the MAWS STARTUP system message appears on the display. However, it takes more than a minute to reach this stage in the procedure.

While this problem is not critical for laboratory testing, it is obviously a safety hazard for the flight trials, since system initialization will occur while the aircraft is on the ground and the system will be radiating through the antenna. While the most desirable solution would be to redesign the powerup configuration through the software, this solution is not feasible due to time and money constraints.

The best feasible solution was to provide a switch that could control the pulsing of the SSPA. This TX on/off switch was placed before the PRFPW control signal input to the SSPA. When this switch is off, there is no pulsing signal to the SSPA. When this switch is on, the PRFPW control signal operates normally. Figure 11 shows this switch as well as the switch described in Section 3.1. In the Figure, the 2.5 MHz feedthrough switch is shown in the "send pulse" position, and the powerup protection switch is in the "TX ON" position.

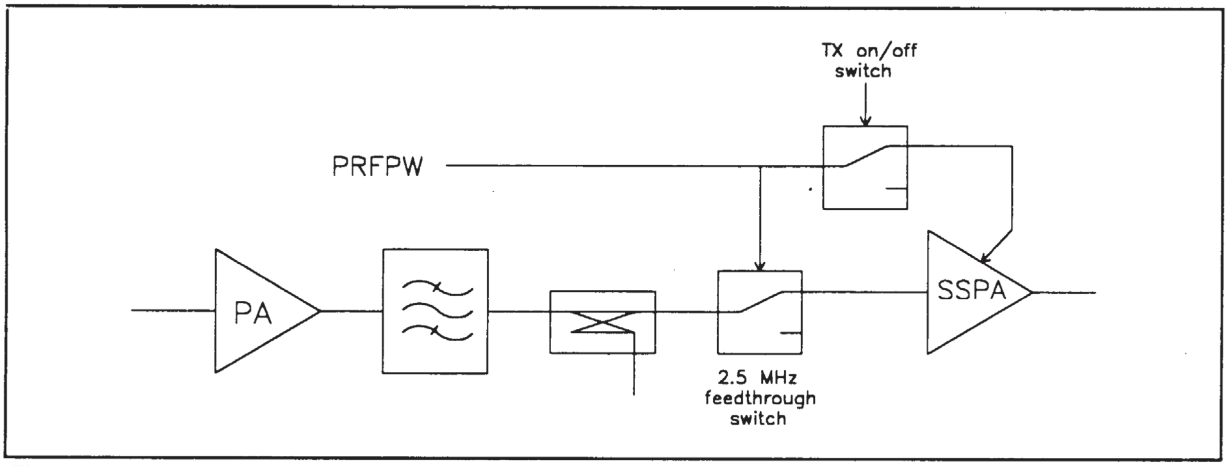

Figure 11 Implementation of the 2.5 MHz Feedthrough and Powerup Protection Switches

The system was tested with the new switch in place, and operates as designed. Control of this switch was added to the pilot interface. During the flight trials the system will initialize on the ground, and will quickly reach its normal operating state. For added safety, however, the TX on/off switch should not be turned on until the aircraft is airborne rather than simply turning it on after initialization. This will preclude any problems that may occur if the aircraft power drops out and the system reinitializes while still on the ground. The pilot will be responsible, then, for turning the switch on after takeoff.

4.0 SUMMARY

The DREO Experimental Missile Approach Warning System transceiver and accompanying data recorder provide a platform for collecting information and experimenting with different radar parameters. This report has described the laboratory tests performed on the transceiver and the specifications achieved. Table VII compares some of the desired performance specifications with those that were actually achieved.

Parameter	*Desired specifications*	*Specifications achieved in system*
Output Power	≥ 200 W peak	≥ 200 W peak at all but one frequency.
RF Frequency	Equal to programmed frequency	Equal to programmed frequency
Harmonic Level of Transmitted Signal	70 dB below the fundamental	Worst harmonic at -43 dBc. Typical 2nd harmonics at -59 dBc, and typical 3rd harmonics at -50 dBc.
Intermodulation Products in Transmitted Signal measured on spectrum analyzer	70 dB below the fundamental	Worst IM product at -22 dBc. Typical IM products at -35 dBc.
Intermodulation Products from IF mixers and amplifiers measured in two tone test	70 dB below the fundamental	Worst IM product at -40 dBc. Typical IM products at -45 dBc.
Noise Figure of Receive Chain	≤ 3 dB	2.56 dB for channel 1 1.51 dB for channel 2
Frequency Response of the Receive Chain	≤ 1 dB variation in response across the band	≤ 1.5 dB variation in response across the band
Image Suppression	70 dB	> 65 dB

Analysis of the system has allowed DREO to identify weaknesses in the translation of the theoretical performance calculations to the values achievable in a physical system. The most serious problem with the current version of the DREO experimental MAWS transceiver is that the suppression of intermodulation products is not high enough. If implemented in a complete missile approach warning system, intermodulation products at the current levels could create unacceptably high false alarm rates. Modification of the transceiver is underway to rectify this problem. Although harmonics in the transmitted signal are also quite high, adequate suppression can be readily achieved by placing an additional filter at the output just before the antenna, at the cost of slightly decreasing the transmitted power.

REFERENCES

[1] V. Manassewitsch, Frequency Synthesizers, Theory and Design, John Wiley and Sons, Inc., New York, 1980.

[2] D. Cheadle, "Selecting Mixers for Best Intermod Performance", Watkins-Johnson Company Catalogue, 1990.

[3] M. Skolnik, Radar Handbook, McGraw-Hill, Inc., New York, 1970, p. 2-29.

[4] P.Nguyen, E.Dekker, and J.Linton, "Technical Manual: MAWS System", MPB Technologies Report MPBT-SO347E-TM-001-01, January 1993.

[5] J.M. Beaulieu, K.Lazare, J.Linton, and P. Nguyen, "Technical Manual: C/DAQU System", MPB Technologies Report MPBT-SO350E-TM-001-01, February 1993.

[6] J.M. Beaulieu, K.Lazare, J.Linton, P. Nguyen, and W.Wu, "Operator's Manual: MAWS and C/DAQU System", MPB Technologies Report MPBT-SO350E-OM-001-01, February, 1993.

[7] P.Nguyen and M.McDougall, "DREO Missile Approach Warning System (MAWS) Detailed Design Report", MPB Technologies Report for DSS W7714-0-9423, June 1991.

[8] G. Rempel, G. Haslam, "A Digital Demodulation Scheme for use in a High Dynamic Range Radar System", Canadian Conference on Electrical and Computer Engineering, Vol I, September 1991, pp 18.4.1-18.4.4.

LIST OF ACRONYMS

A/D	Analog to Digital (converter)
C/DAQU	Controller/Data Acquisition Unit
CME	Cabin Mounted Equipment
CW	Continuous Wave
EPA	External Payload Assembly
FFT	Fast Fourier Transform
FIR filter	Finite Impulse Response filter
IAR	Institute for Aerospace Research
IF	Intermediate Frequency
IM product	Intermodulation product
MAWS	Missile Approach Warning System
PA	Power Amplifier
PRF	Pulse Repetition Frequency
PRI	Pulse Repetition Interval
SNR	Signal to Noise Ratio
SSPA	Solid State Power Amplifier
STC	Sensitivity Time Control

Appendix A
Single Tone Test Spectra

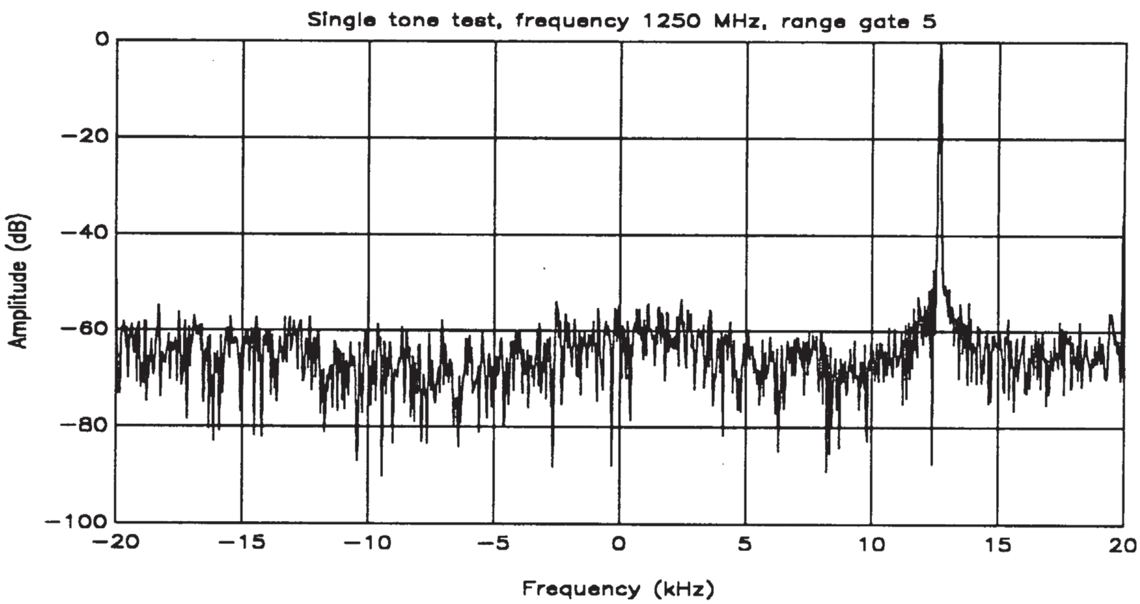

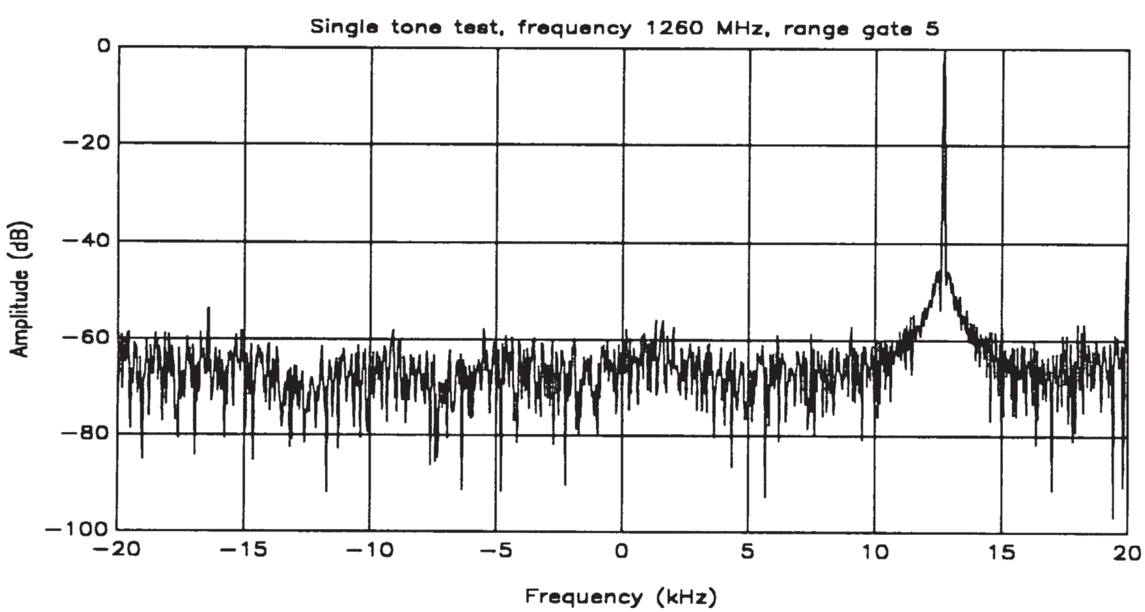

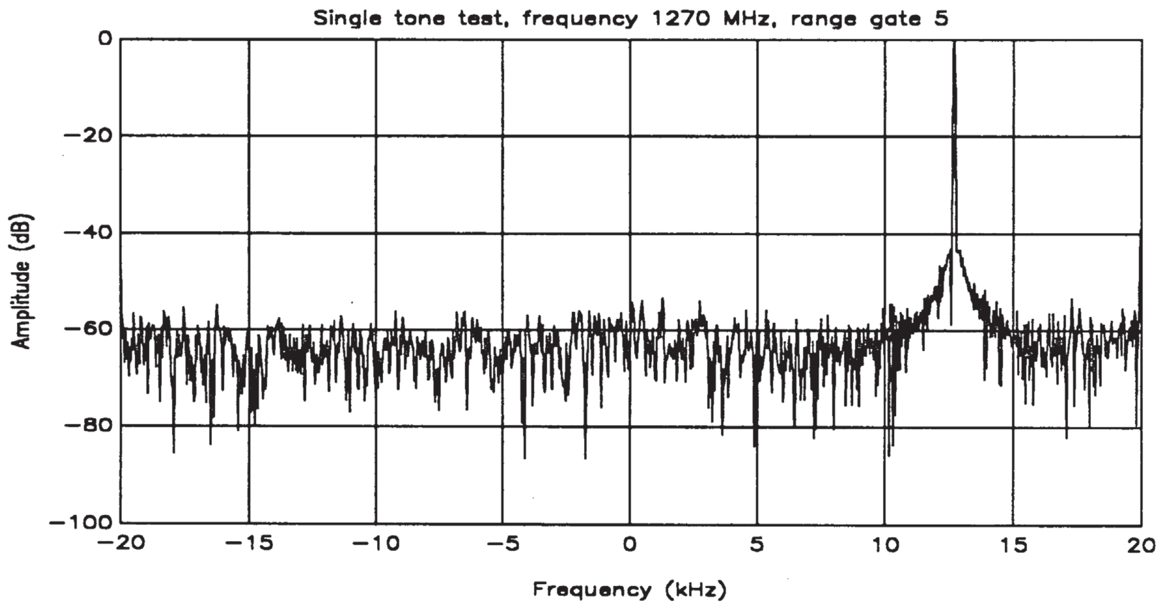
Single tone test, frequency 1270 MHz, range gate 5
0
−20
−40
−60
−80
−100
Amplitude (dB)
−20
−15
−10
−5
0
5
10
15
20
Frequency (kHz)

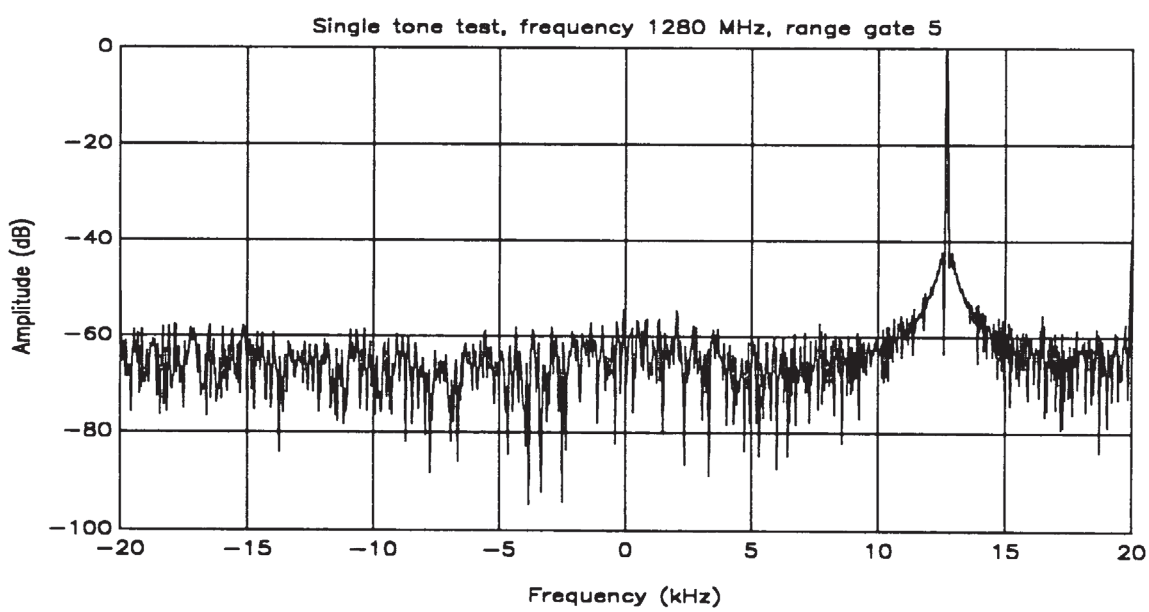
Single tone test, frequency 1280 MHz, range gate 5
0
−20
−40
−60
−80
−100
Amplitude (dB)
−20
−15
−10
−5
0
5
10
15
20
Frequency (kHz)

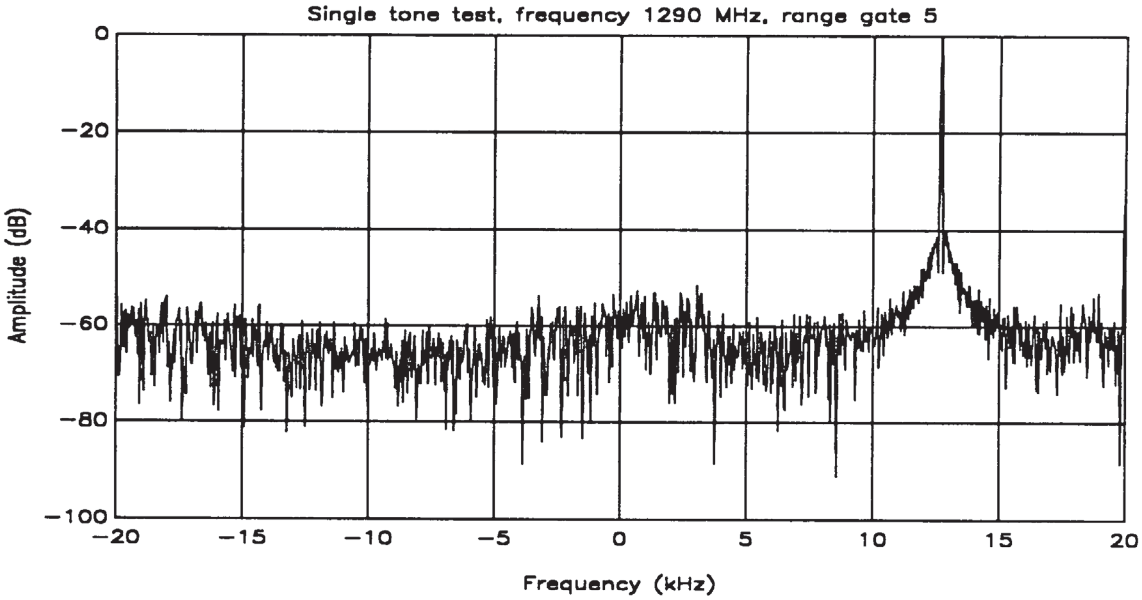
Single tone test, frequency 1290 MHz, range gate 5
Amplitude (dB)
0
−20
−40
−60
−80
−100
−20
−15
−10
−5
0
5
10
15
20
Frequency (kHz)

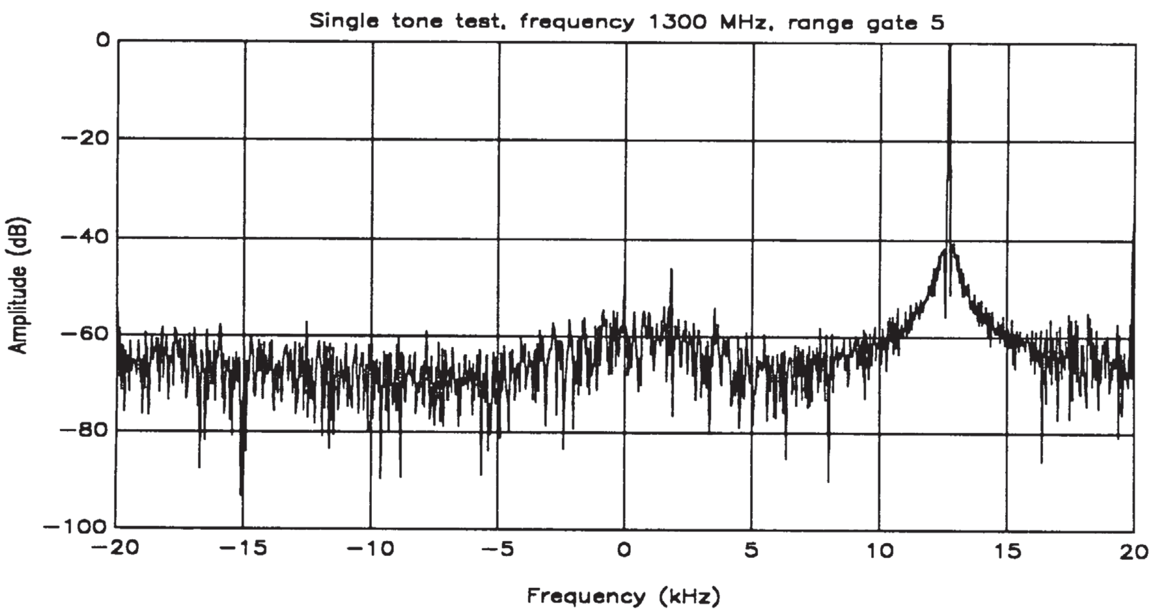
Single tone test, frequency 1300 MHz, range gate 5
Amplitude (dB)
0
−20
−40
−60
−80
−100
−20
−15
−10
−5
0
5
10
15
20
Frequency (kHz)

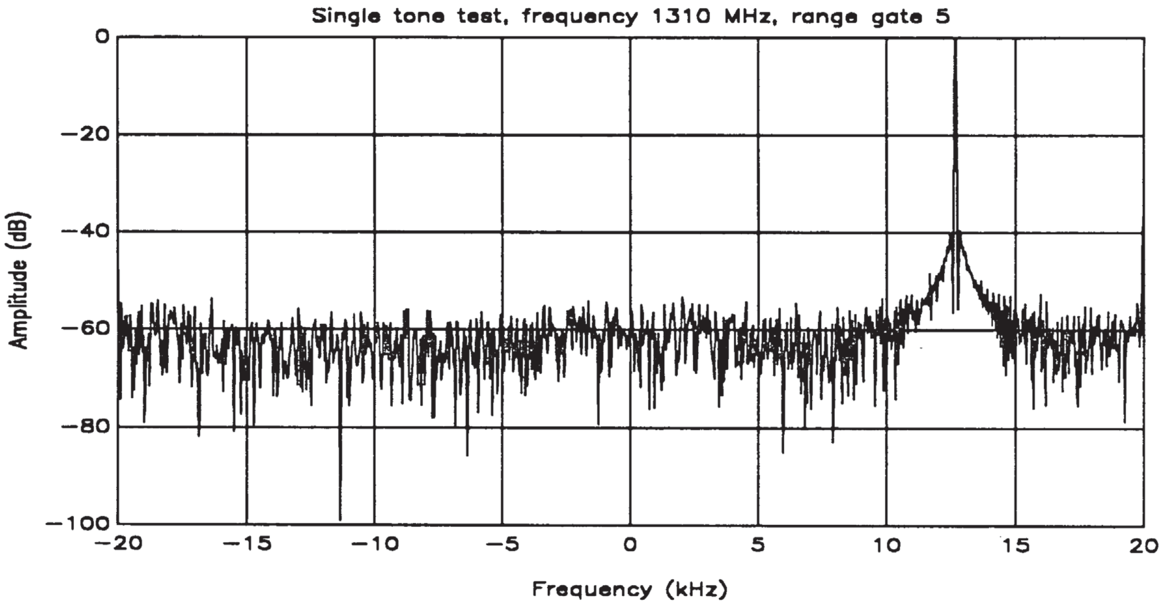
Single tone test, frequency 1310 MHz, range gate 5
Amplitude (dB)
0
−20
−40
−60
−80
−100
−20
−15
−10
−5
0
5
10
15
20
Frequency (kHz)

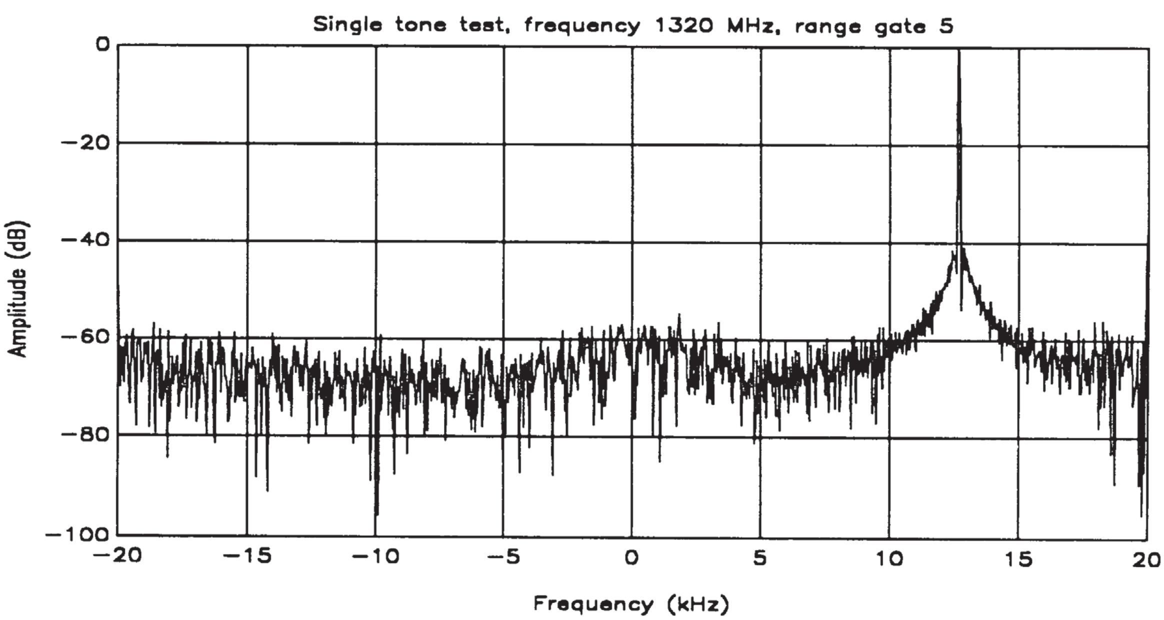
Single tone test, frequency 1320 MHz, range gate 5
Amplitude (dB)
0
−20
−40
−60
−80
−100
−20
−15
−10
−5
0
5
10
15
20
Frequency (kHz)

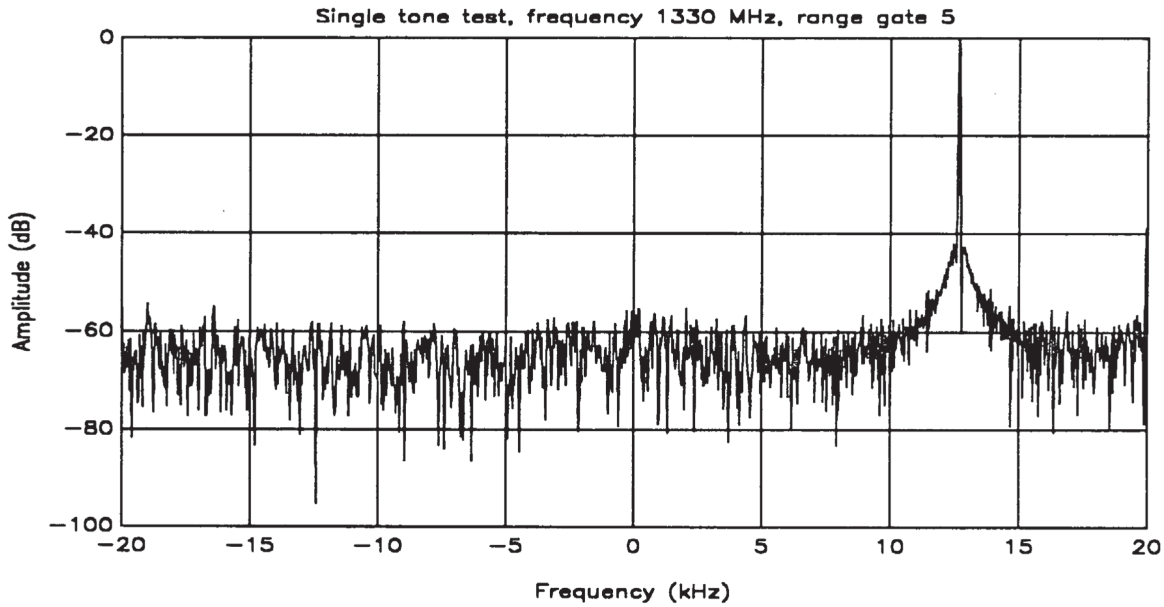
Single tone test, frequency 1330 MHz, range gate 5
Amplitude (dB)
0
−20
−40
−60
−80
−100
−20
−15
−10
−5
0
5
10
15
20
Frequency (kHz)

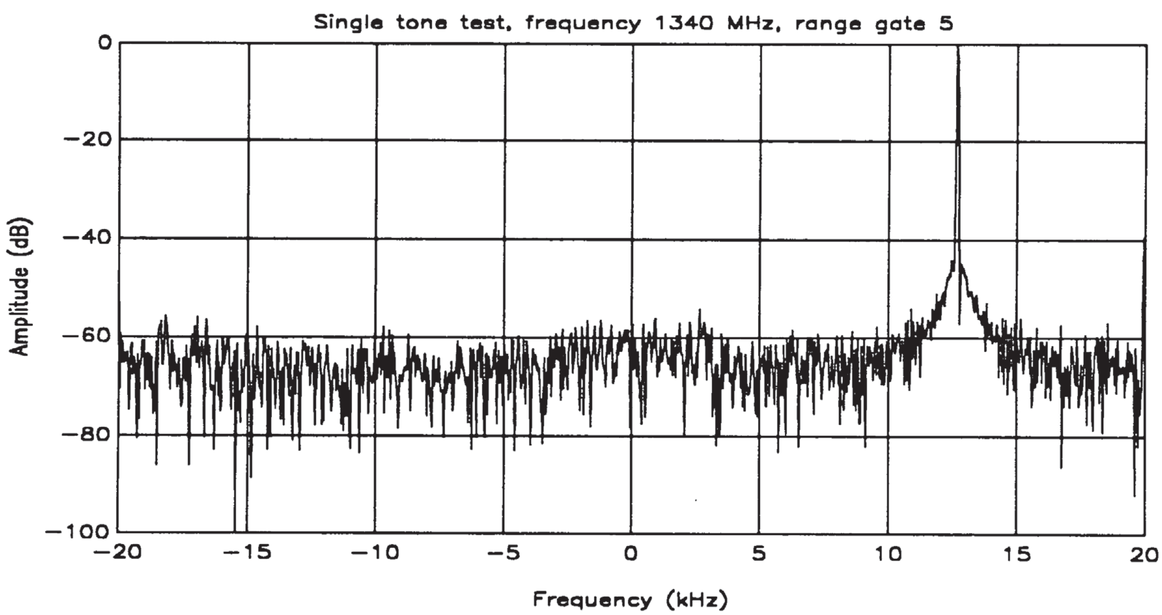
Single tone test, frequency 1340 MHz, range gate 5
Amplitude (dB)
0
−20
−40
−60
−80
−100
−20
−15
−10
−5
0
5
10
15
20
Frequency (kHz)

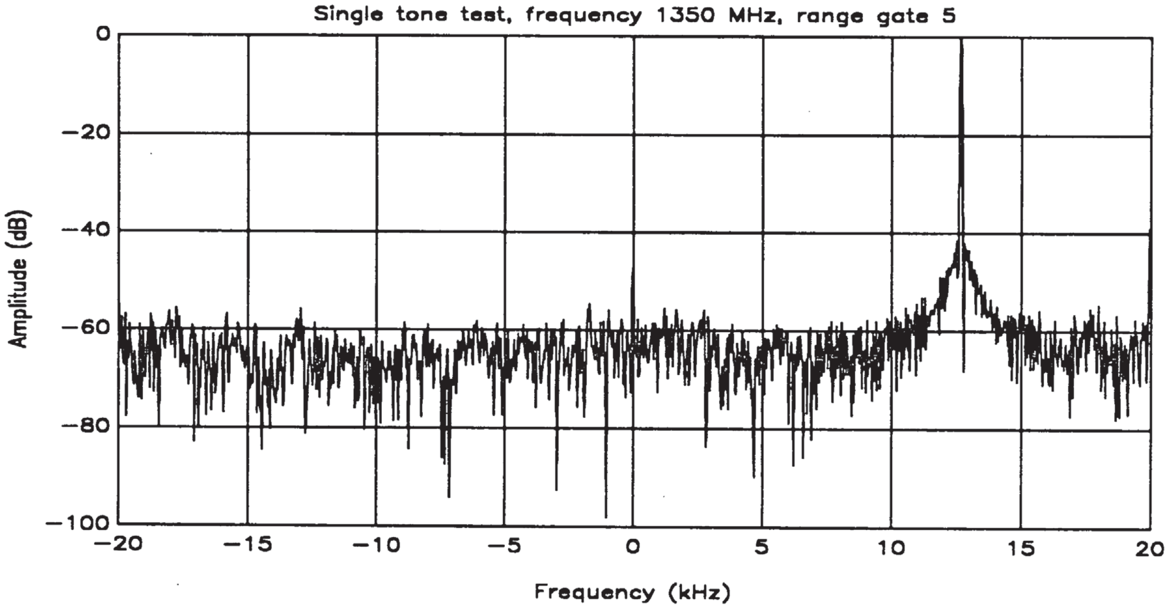
Single tone test, frequency 1350 MHz, range gate 5
Amplitude (dB)
0
−20
−40
−60
−80
−100
−20
−15
−10
−5
0
5
10
15
20
Frequency (kHz)

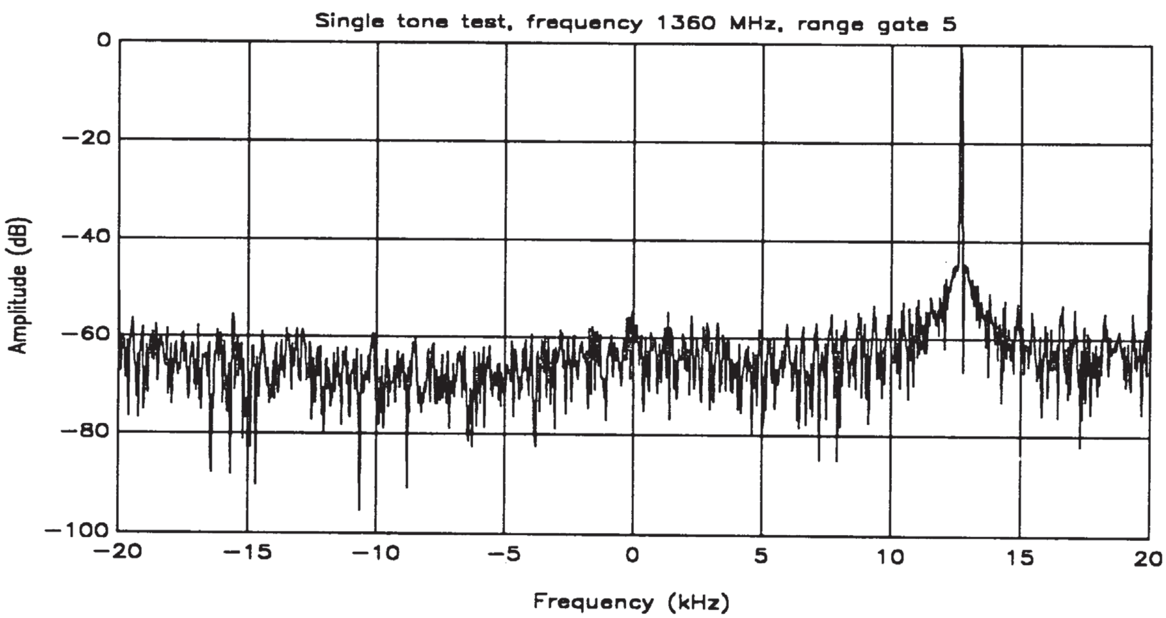
Single tone test, frequency 1360 MHz, range gate 5
Amplitude (dB)
0
−20
−40
−60
−80
−100
−20
−15
−10
−5
0
5
10
15
20
Frequency (kHz)

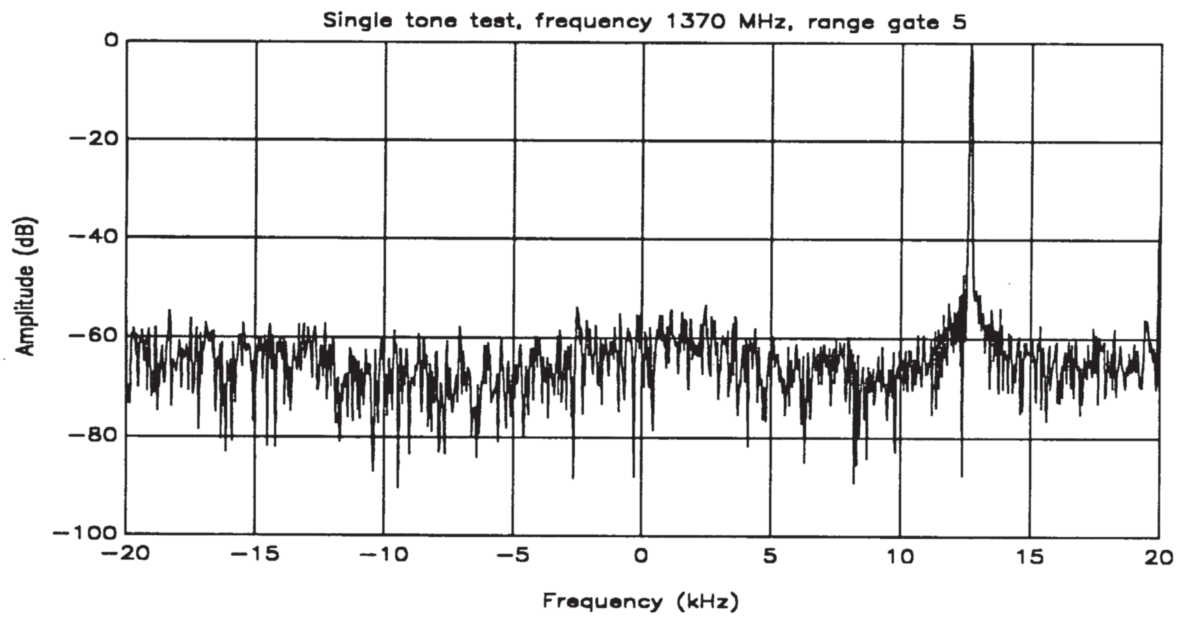
Single tone test, frequency 1370 MHz, range gate 5
Amplitude (dB)
0
−20
−40
−60
−80
−100
−20
−15
−10
−5
0
5
10
15
20
Frequency (kHz)

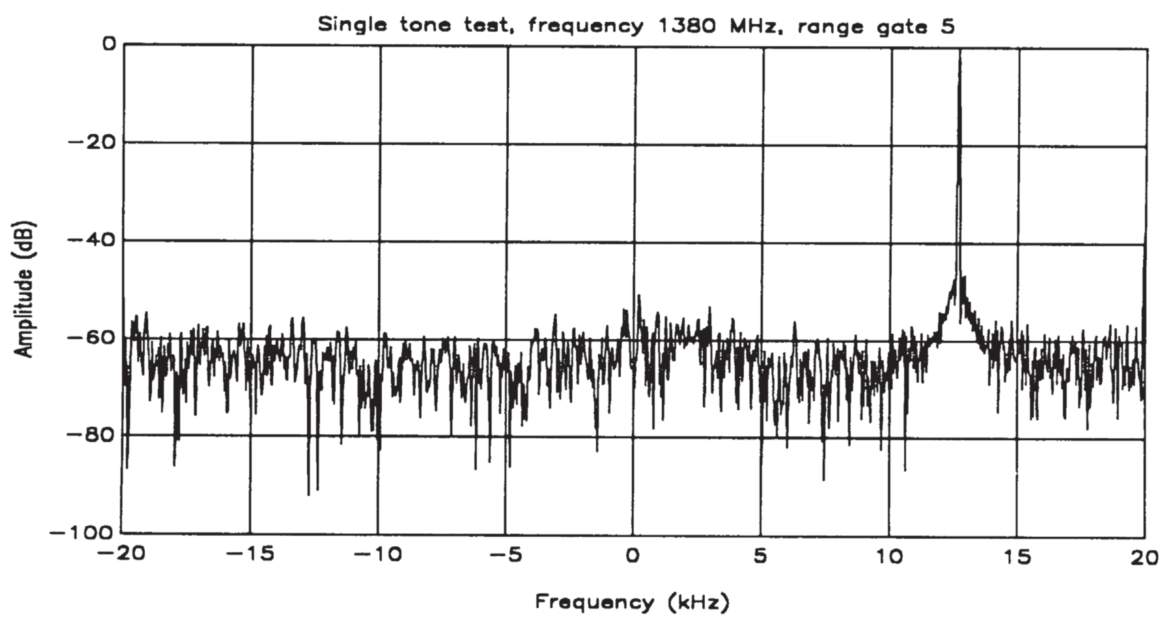
Single tone test, frequency 1380 MHz, range gate 5
Amplitude (dB)
0
−20
−40
−60
−80
−100
−20
−15
−10
−5
0
5
10
15
20
Frequency (kHz)

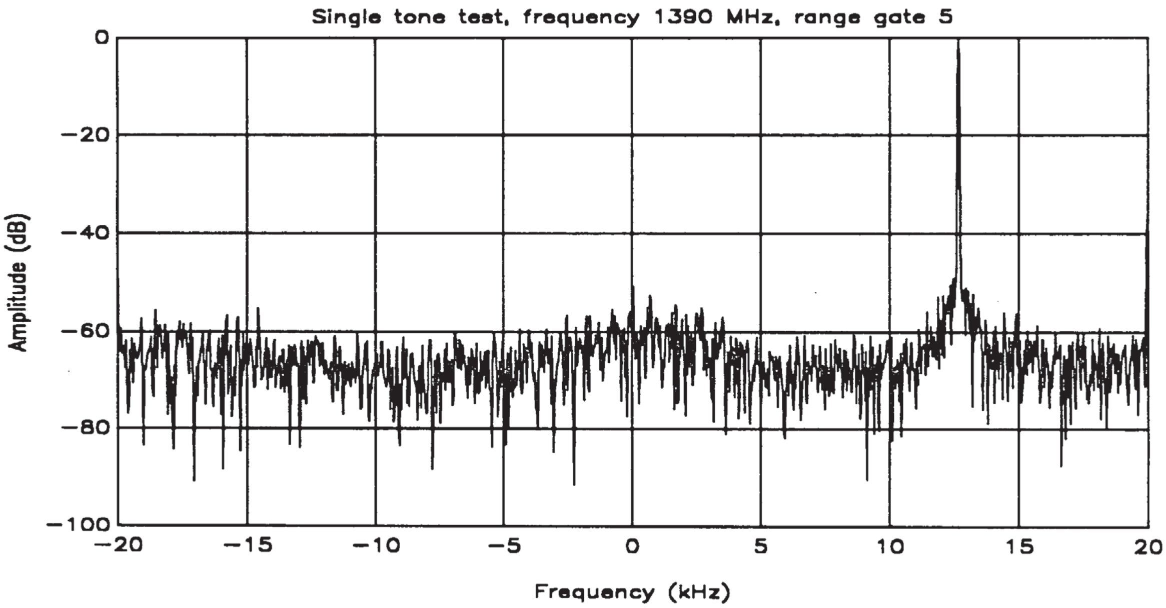
Single tone test, frequency 1390 MHz, range gate 5
0
−20
−40
−60
−80
−100
Amplitude (dB)
−20
−15
−10
−5
0
5
10
15
20
Frequency (kHz)

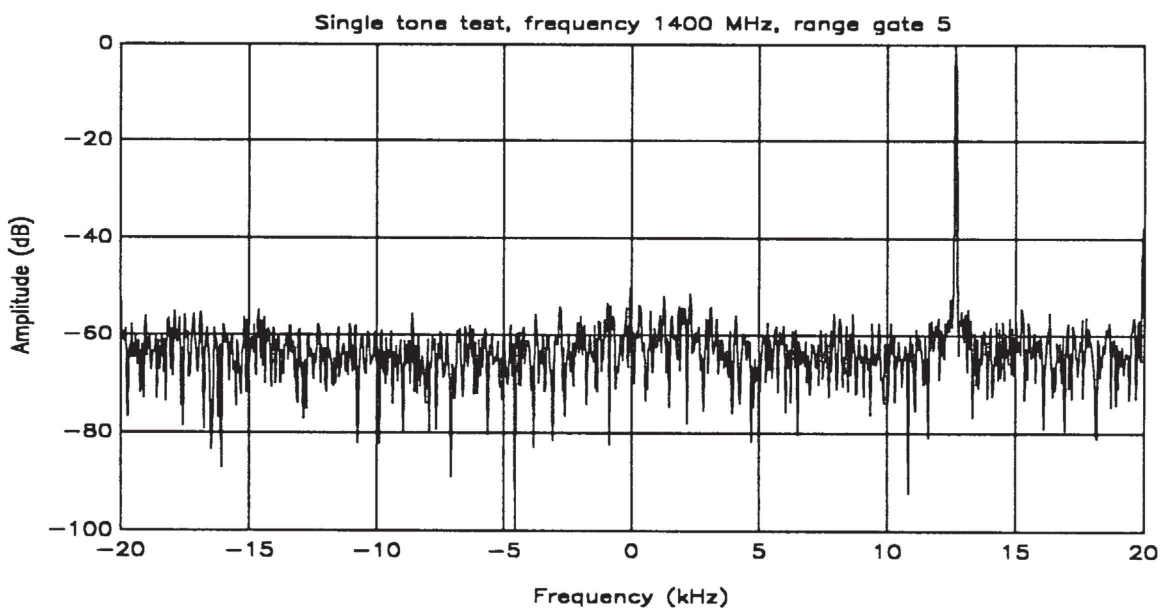
Single tone test, frequency 1400 MHz, range gate 5
0
−20
−40
−60
−80
−100
Amplitude (dB)
−20
−15
−10
−5
0
5
10
15
20
Frequency (kHz)

Appendix B
Two Tone Test Spectra

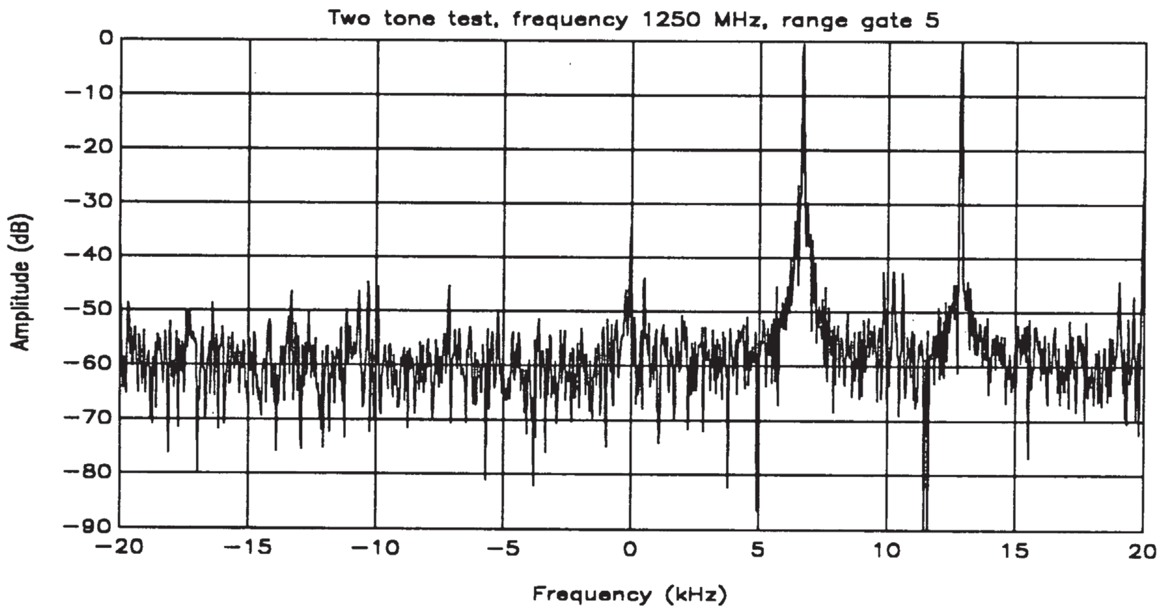

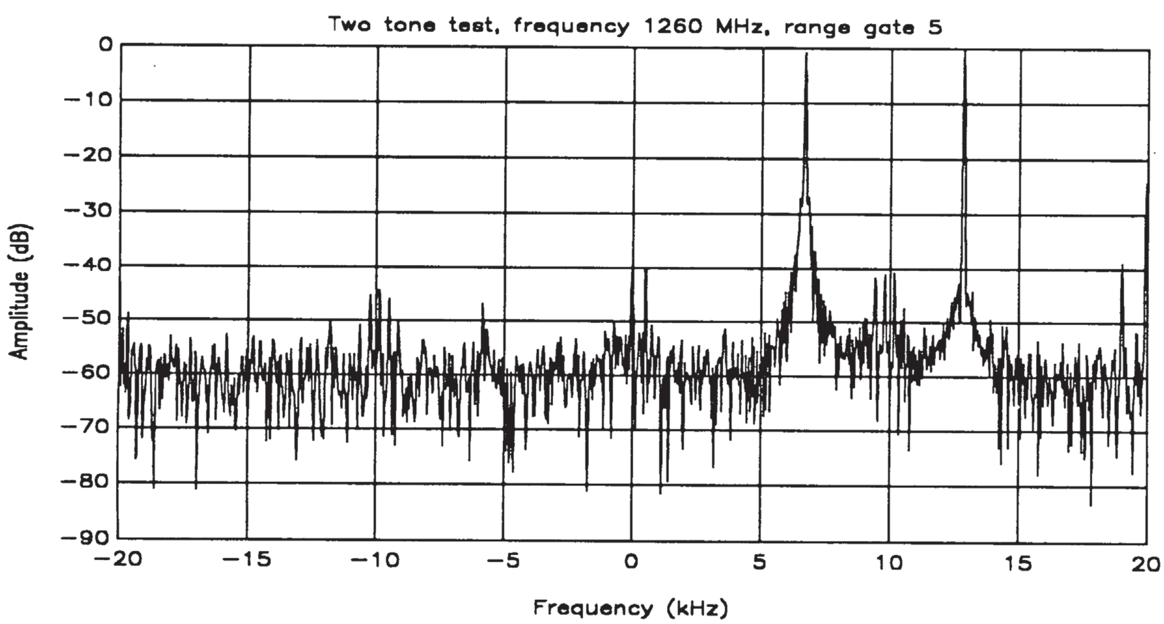

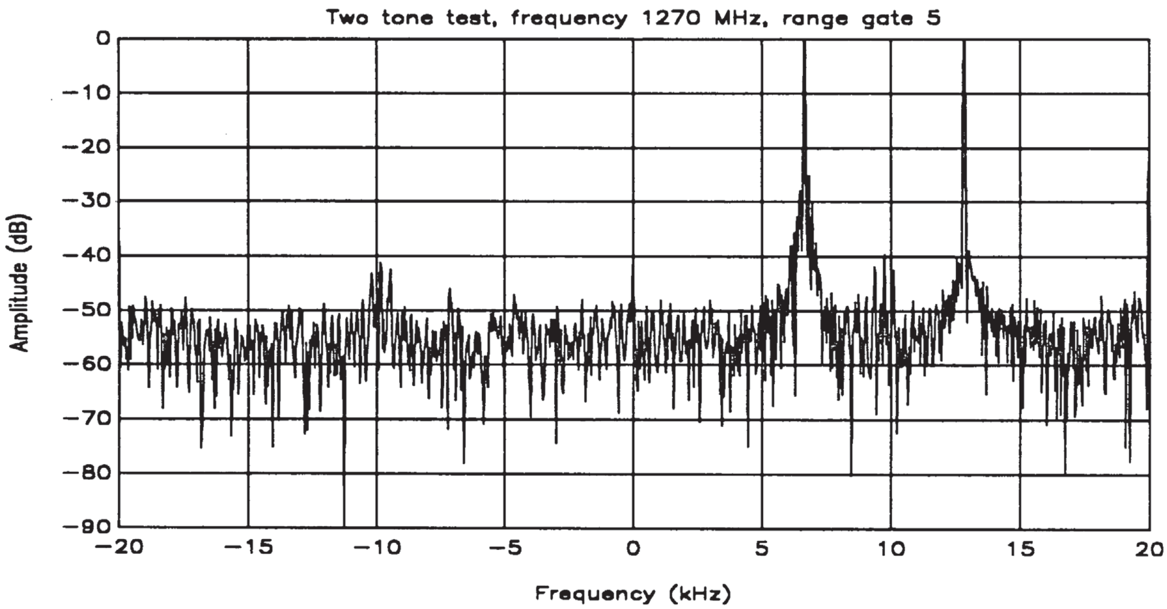
Two tone test, frequency 1270 MHz, range gate 5
Amplitude (dB)
0
−10
−20
−30
−40
−50
−60
−70
−80
−90
−20
−15
−10
−5
0
5
10
15
20
Frequency (kHz)

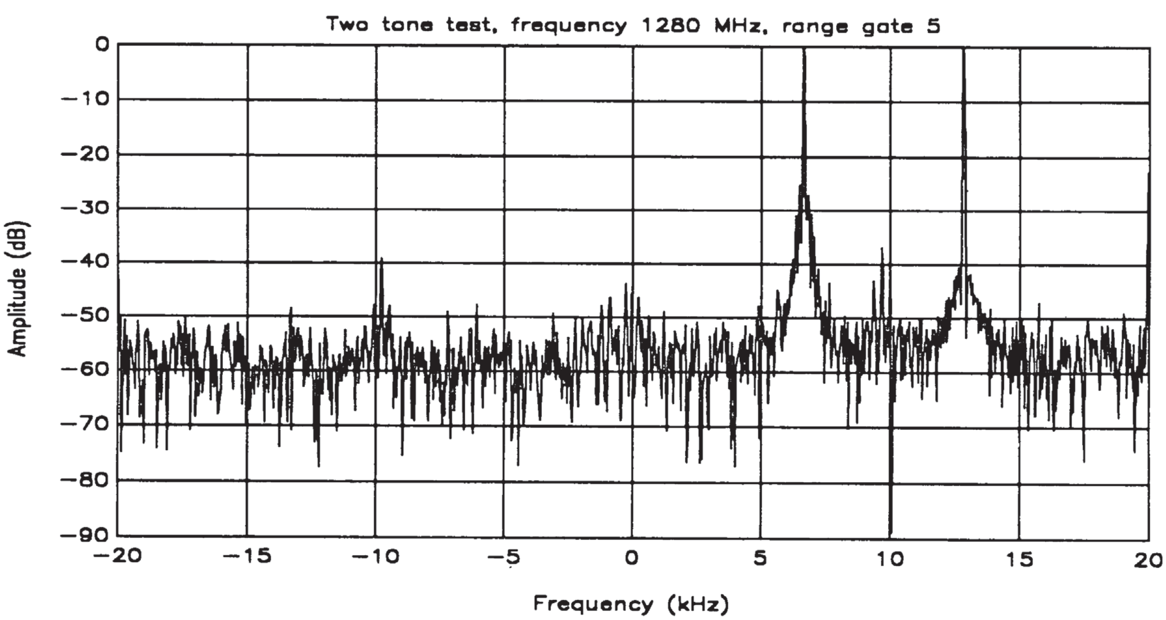
Two tone test, frequency 1280 MHz, range gate 5
Amplitude (dB)
0
−10
−20
−30
−40
−50
−60
−70
−80
−90
−20
−15
−10
−5
0
5
10
15
20
Frequency (kHz)

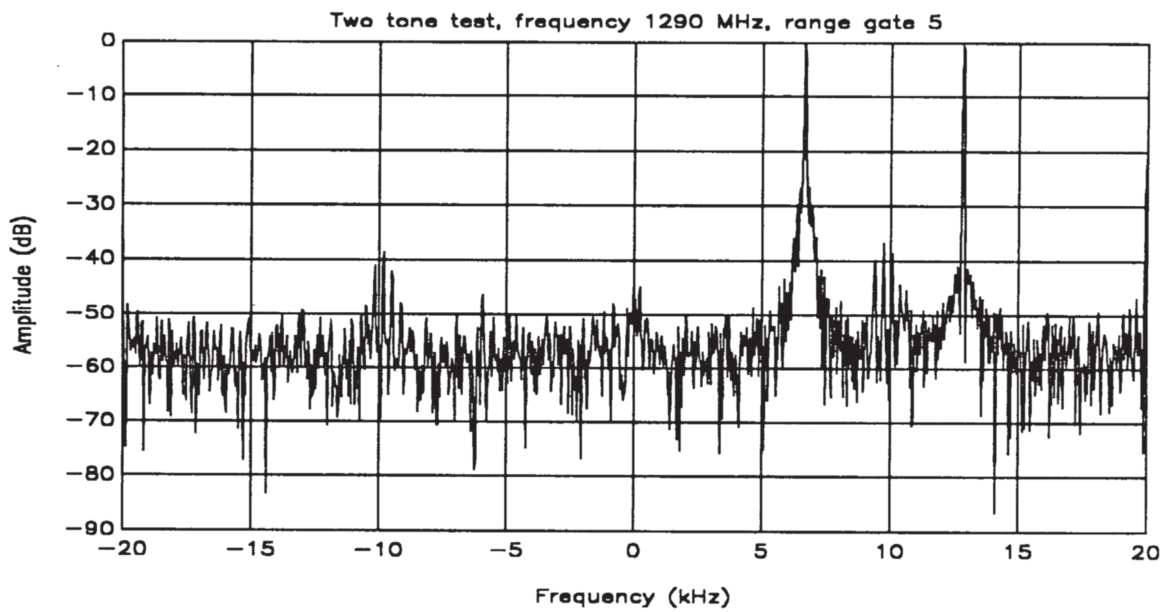
Two tone test, frequency 1290 MHz, range gate 5
Amplitude (dB)
0
−10
−20
−30
−40
−50
−60
−70
−80
−90
−20
−15
−10
−5
0
5
10
15
20
Frequency (kHz)

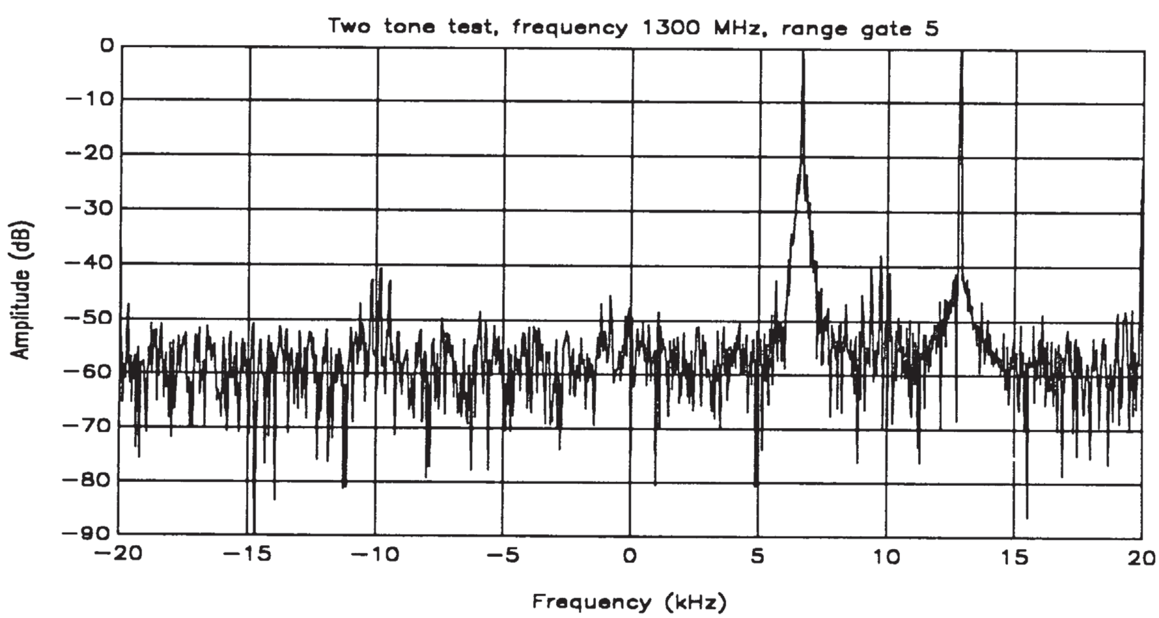
Two tone test, frequency 1300 MHz, range gate 5
Amplitude (dB)
0
−10
−20
−30
−40
−50
−60
−70
−80
−90
−20
−15
−10
−5
0
5
10
15
20
Frequency (kHz)

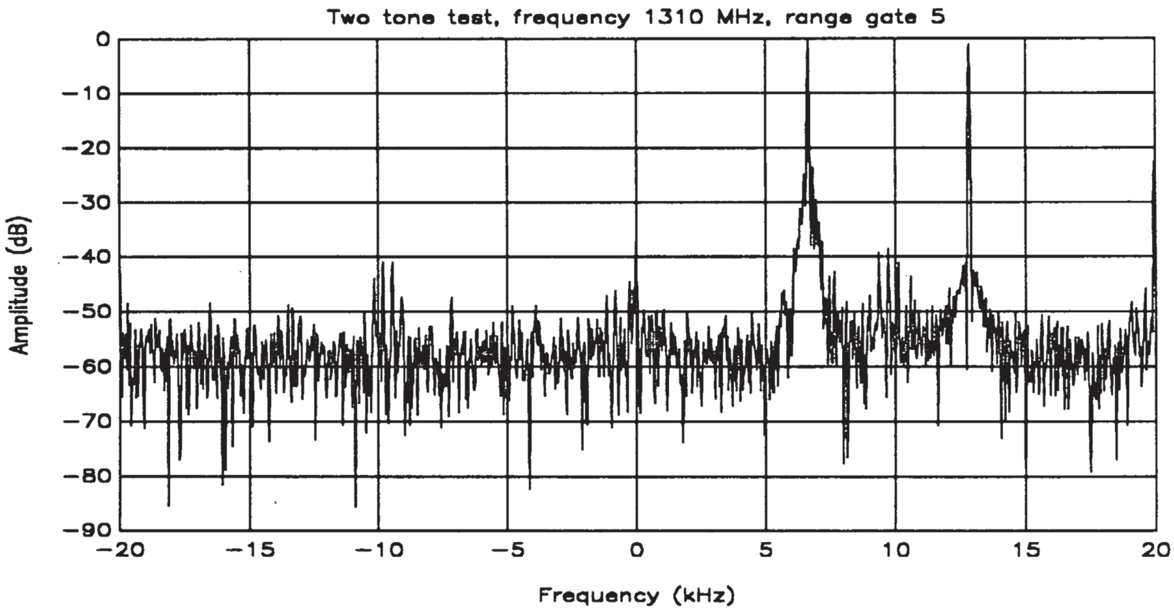
Two tone test, frequency 1310 MHz, range gate 5
Amplitude (dB)
0
−10
−20
−30
−40
−50
−60
−70
−80
−90
−20
−15
−10
−5
0
5
10
15
20
Frequency (kHz)

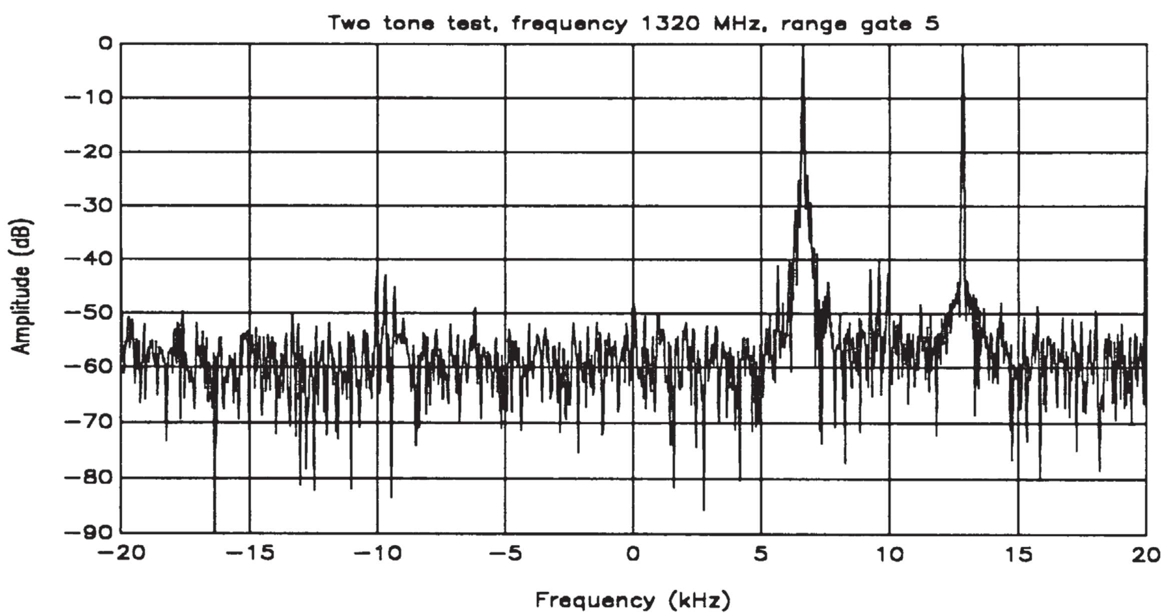
Two tone test, frequency 1320 MHz, range gate 5
Amplitude (dB)
0
−10
−20
−30
−40
−50
−60
−70
−80
−90
−20
−15
−10
−5
0
5
10
15
20
Frequency (kHz)

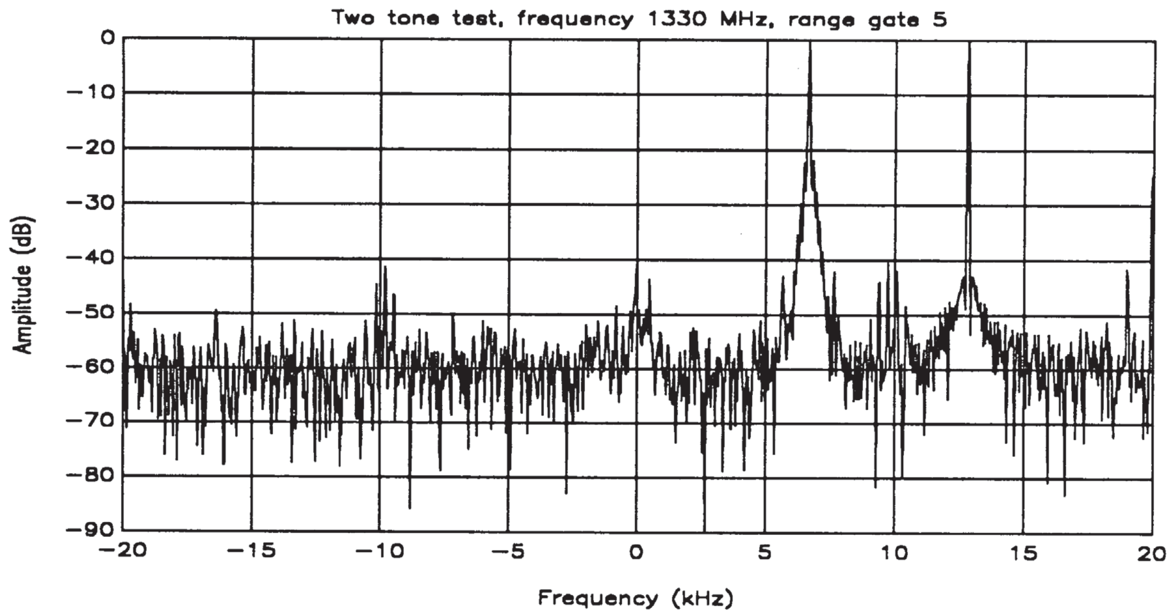
Two tone test, frequency 1330 MHz, range gate 5
0
−10
−20
−30
−40
−50
−60
−70
−80
−90
Amplitude (dB)
−20
−15
−10
−5
0
5
10
15
20
Frequency (kHz)

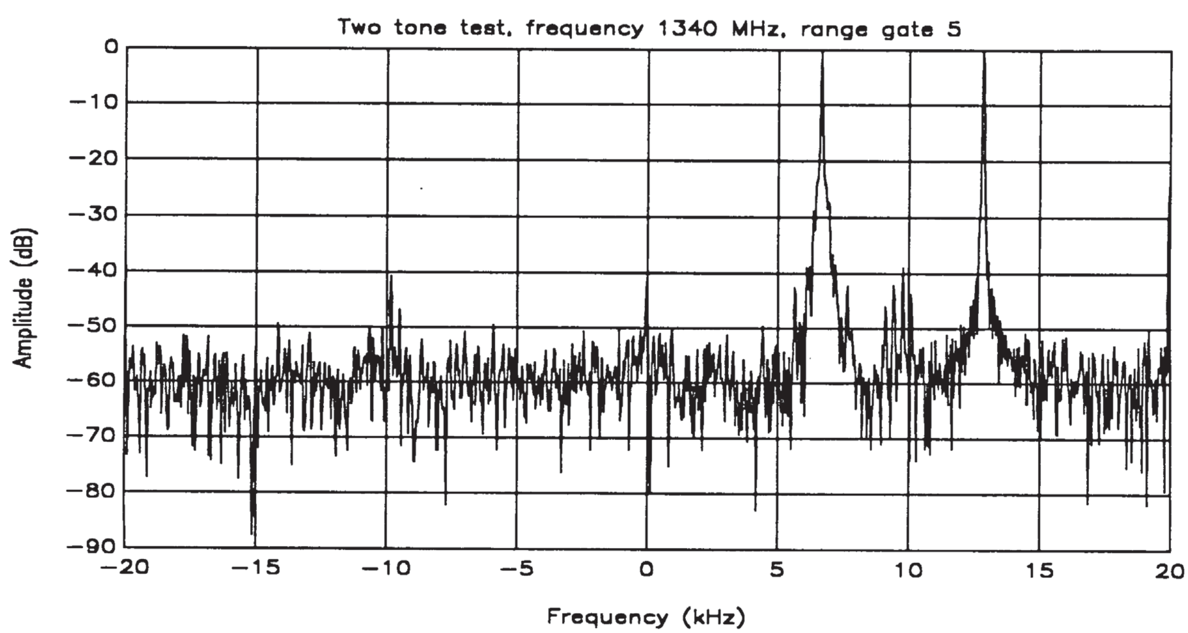
Two tone test, frequency 1340 MHz, range gate 5
0
−10
−20
−30
−40
−50
−60
−70
−80
−90
Amplitude (dB)
−20
−15
−10
−5
0
5
10
15
20
Frequency (kHz)

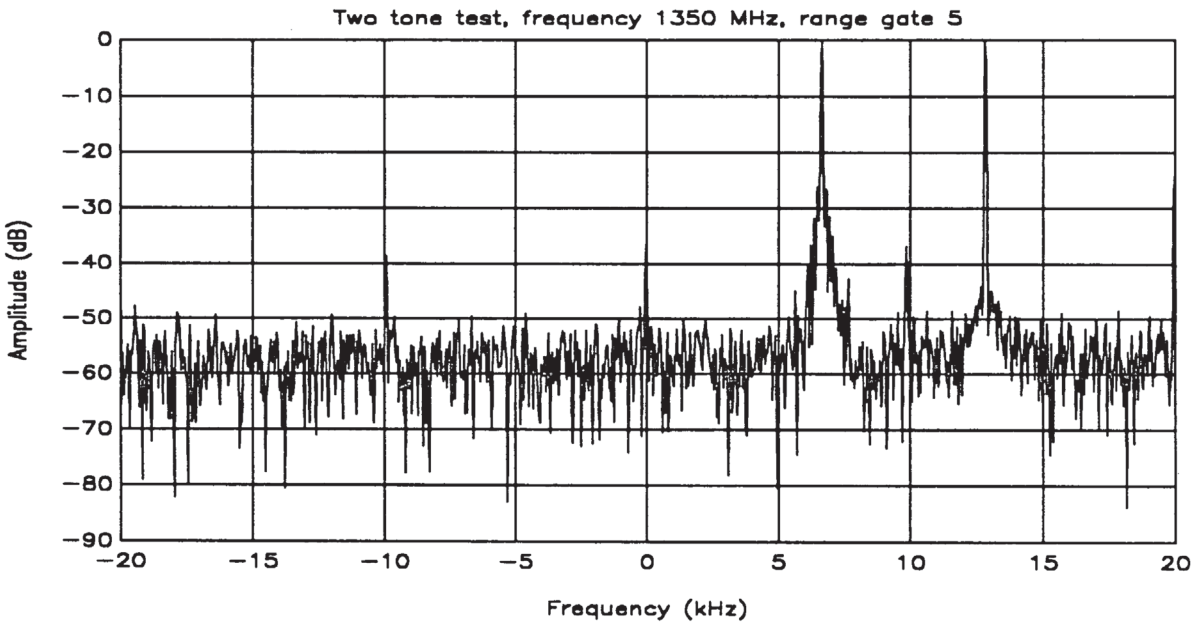
Two tone test, frequency 1350 MHz, range gate 5
Amplitude (dB)
Frequency (kHz)
0
−10
−20
−30
−40
−50
−60
−70
−80
−90
−20
−15
−10
−5
0
5
10
15
20

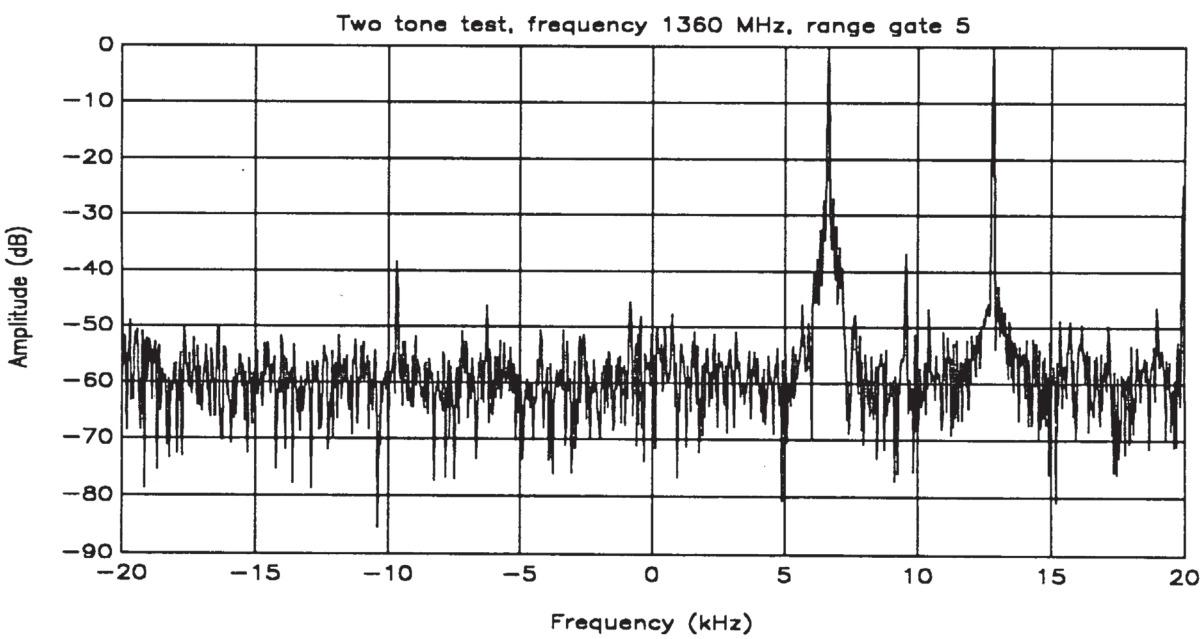
Two tone test, frequency 1360 MHz, range gate 5
Amplitude (dB)
Frequency (kHz)
0
−10
−20
−30
−40
−50
−60
−70
−80
−90
−20
−15
−10
−5
0
5
10
15
20

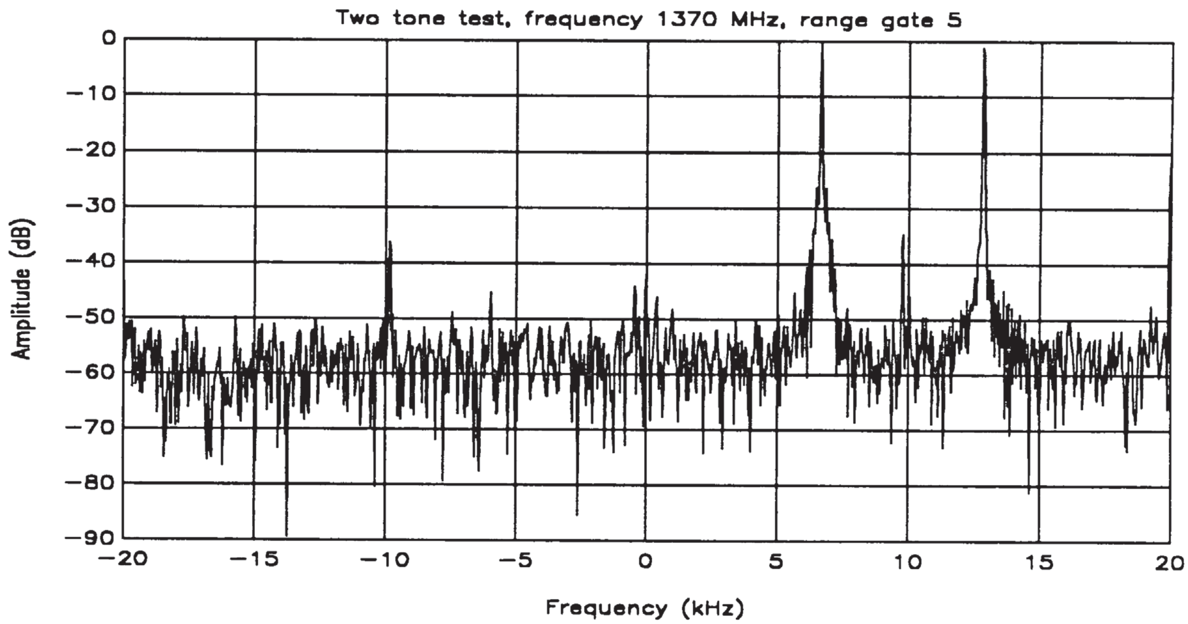
Two tone test, frequency 1370 MHz, range gate 5
Amplitude (dB)
0
−10
−20
−30
−40
−50
−60
−70
−80
−90
−20
−15
−10
−5
0
5
10
15
20
Frequency (kHz)

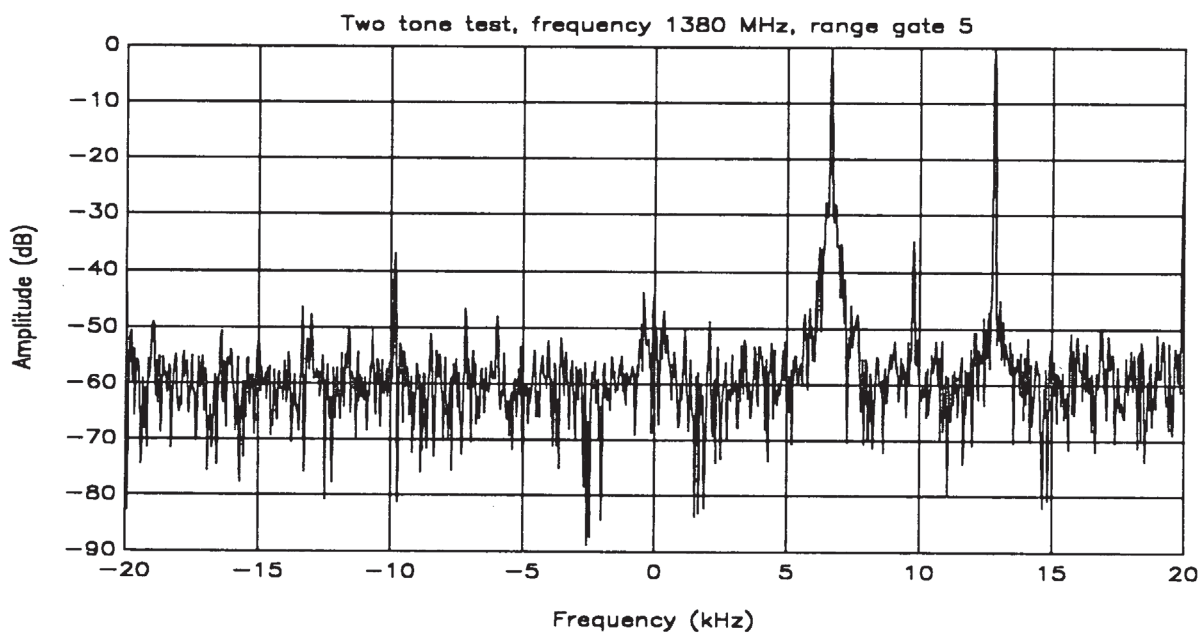
Two tone test, frequency 1380 MHz, range gate 5
Amplitude (dB)
0
−10
−20
−30
−40
−50
−60
−70
−80
−90
−20
−15
−10
−5
0
5
10
15
20
Frequency (kHz)

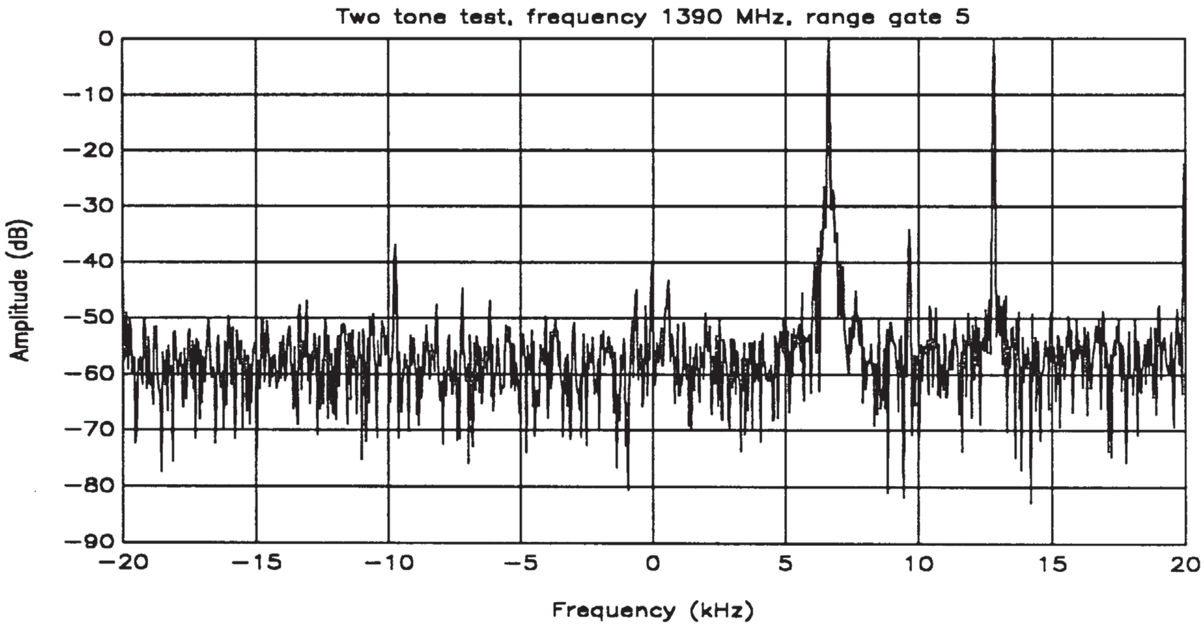
Two tone test, frequency 1390 MHz, range gate 5
Amplitude (dB)
Frequency (kHz)
0
−10
−20
−30
−40
−50
−60
−70
−80
−90
−20
−15
−10
−5
0
5
10
15
20

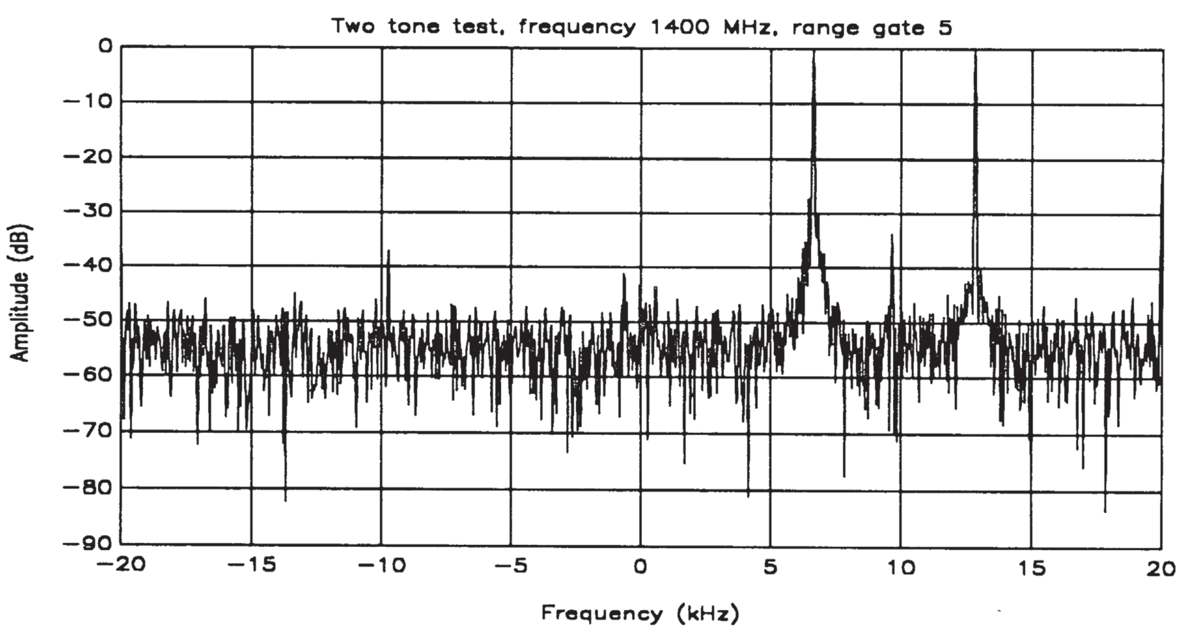
Two tone test, frequency 1400 MHz, range gate 5
Amplitude (dB)
Frequency (kHz)
0
−10
−20
−30
−40
−50
−60
−70
−80
−90
−20
−15
−10
−5
0
5
10
15
20

DOCUMENT CONTROL DATA

(Security classification of title, body of abstract and indexing annotation must be entered when the overall document is classified)

1. ORIGINATOR (the name and address of the organization preparing the document. Organizations for whom the document was prepared, e.g. Establishment sponsoring a contractor's report, or tasking agency, are entered in section 8.)

Defence Research Establishment Ottawa
Ottawa, ON
K1A 0Z4

2. SECURITY CLASSIFICATION (overall security classification of the document. including special warning terms if applicable)

UNCLASSIFIED

3. TITLE (the complete document title as indicated on the title page. Its classification should be indicated by the appropriate abbreviation (S,C or U) in parentheses after the title.)

Laboratory Testing Results for the DREO Experimental MAWS Transceiver (U)

4. AUTHORS (Last name, first name, middle initial)

Campbell, Lori L., Rempel, Glen E., Robinson, Robert W.

5. DATE OF PUBLICATION (month and year of publication of document)

November 1993

6a. NO. OF PAGES (total containing information. Include Annexes, Appendices, etc.)

47

6b. NO. OF REFS (total cited in document)

8

7. DESCRIPTIVE NOTES (the category of the document, e.g. technical report, technical note or memorandum. If appropriate, enter the type of report, e.g. interim, progress, summary, annual or final. Give the inclusive dates when a specific reporting period is covered.)

Technical Report

8. SPONSORING ACTIVITY (the name of the department project office or laboratory sponsoring the research and development. Include the address.)

9a. PROJECT OR GRANT NO. (if appropriate, the applicable research and development project or grant number under which the document was written. Please specify whether project or grant)

021LA

9b. CONTRACT NO. (if appropriate, the applicable number under which the document was written)

10a. ORIGINATOR'S DOCUMENT NUMBER (the official document number by which the document is identified by the originating activity. This number must be unique to this document.)

DREO REPORT 1205

10b. OTHER DOCUMENT NOS. (Any other numbers which may be assigned this document either by the originator or by the sponsor)

11. DOCUMENT AVAILABILITY (any limitations on further dissemination of the document, other than those imposed by security classification)

(X) Unlimited distribution
( ) Distribution limited to defence departments and defence contractors; further distribution only as approved
( ) Distribution limited to defence departments and Canadian defence contractors; further distribution only as approved
( ) Distribution limited to government departments and agencies; further distribution only as approved
( ) Distribution limited to defence departments; further distribution only as approved
( ) Other (please specify):

12. DOCUMENT ANNOUNCEMENT (any limitation to the bibliographic announcement of this document. This will normally correspond to the Document Availabilty (11). However, where further distribution (beyond the audience specified in 11) is possible, a wider announcement audience may be selected.)

13. ABSTRACT (a brief and factual summary of the document. It may also appear elsewhere in the body of the document itself. It is highly desirable that the abstract of classified documents be unclassified. Each paragraph of the abstract shall begin with an indication of the security classification of the information in the paragraph (unless the document itself is unclassified) represented as (S), (C), or (U). It is not necessary to include here abstracts in both offical languages unless the text is bilingual).

An experimental transceiver for a radar-based Missile Approach Warning System (MAWS) was developed at the Defence Research Establishment Ottawa to aid in studying the most effective techniques for design and implementation of such systems. With the help of Canadian industry, the experimental system was completed in November of 1992. The transceiver was designed for airborne use, and will be undergoing flight trials in 1994. The MAWS transceiver is an L-band pulse Doppler radar with frequency agility, multiple pulse repetition frequencies, and pulse coding capabilities.

This report outlines laboratory tests conducted on the experimental DREO MAWS transceiver, and shows performance specifications achieved by the system. These tests were designed to verify critical parameters of the transceiver, while providing a broad base of information that will aid in interpreting data from future flight tests. As well, the information contained in this report serves as a foundation for evaluating improvements made through further design modifications.

14. KEYWORDS, DESCRIPTORS or IDENTIFIERS (technically meaningful terms or short phrases that characterize a document and could be helpful in cataloguing the document. They should be selected so that no security classification is required. Identifiers, such as equipment model designation, trade name, military project code name, geographic location may also be included. If possible keywords should be selected from a published thesaurus. e.g. Thesaurus of Engineering and Scientific Terms (TEST) and that thesaurus-identified. If it is not possible to select indexing terms which are Unclassified, the classification of each should be indicated as with the title.)

Missile Approach Warning System
MAWS
Pulse Doppler Radar